in rectal cancer. *J Clin Oncol* 19(6): 1779-1786, 2001.
29) Schwab M, Zanger UM, Marx C, *et al*: Role of genetic ar nongenetic factors for fluorouracil treatment-related s vere toxicity: a prospective clinical trial by the German 5-FU Toxicity Study Group. *J Clin Oncol* 26(13): 2131-2138, 2008.

Int J Clin Oncol
DOI 10.1007/s10147-011-0348-6

ORIGINAL ARTICLE

Evaluation of safety, pharmacokinetics, and efficacy of vorinostat, a histone deacetylase inhibitor, in the treatment of gastrointestinal (GI) cancer in a phase I clinical trial

Toshihiko Doi · Tetsuya Hamaguchi · Kuniaki Shirao · Kensho Chin · Kiyohiko Hatake · Kazuo Noguchi · Tetsuya Otsuki · Anish Mehta · Atsushi Ohtsu

Received: 25 May 2011 / Accepted: 29 October 2011

Abstract
Background Control of epigenetic changes using histone deacetylase inhibitors (HDACi) is thought to be a promising target in therapy of gastrointestinal (GI) cancer. In this study, we evaluated the safety, pharmacokinetics, and efficacy of two dosing regimens of vorinostat, an oral HDACi, in patients with GI tumors.
Methods Patients received either vorinostat 300 mg bid for 3 consecutive days followed by 4 rest days per cycle ($n = 10$) or vorinostat 400 mg qd for 21 consecutive days per cycle ($n = 6$). Pharmacokinetic parameters were assessed for the first treatment cycle. Efficacy was determined through evaluation of tumors and assessment of treatment response.
Results The median treatment duration of 300 mg bid was 52.0 days and of 400 mg qd was 51.5 days. The most common drug-related adverse events were anorexia, nausea, fatigue, and hyperglycemia. Two patients taking 400 mg qd had dose-limiting toxicities (DLTs) of thrombocytopenia. No patients taking 300 mg bid experienced DLT. Five patients taking 300 mg bid and 2 patients taking 400 mg qd maintained stable disease for >8 weeks, with the maximum duration of 245 days. Mean drug exposure (±SD) was generally higher with 400 mg qd (area under the curve [$AUC_{0-\infty}$] of 7.75 ± 2.79 μM h on Day 1 post-dose) compared with 300 mg bid ($AUC_{0-\infty}$ of 3.94 ± 1.56 μM h on Day 1 post-dose).
Conclusions Vorinostat 300 mg bid for 3 consecutive days followed by 4 days of rest was better tolerated in patients with GI cancer than a higher once daily dose. Additionally, there were patients in both groups who achieved stable disease, most maintaining it for longer than 8 weeks, suggesting vorinostat as a possible active agent in the treatment of GI cancer.

Keywords Histone deacetylase inhibitor (HDACi) · Gastrointestinal cancer · Vorinostat · Suberoylanilide hydroxamic acid (SAHA)

T. Doi (✉) · A. Ohtsu
National Cancer Center Hospital East, Chiba, Japan
e-mail: doi.toshi3@gmail.com

T. Hamaguchi
National Cancer Center, Tokyo, Japan

K. Shirao
Oita University, Oita, Japan

K. Chin · K. Hatake
Cancer Institute Hospital of Japanese Foundation for Cancer Research, Tokyo, Japan

K. Noguchi · T. Otsuki
MSD K.K., Tokyo, Japan

A. Mehta
Merck Sharpe & Dohme Corp, Whitehouse Station, NJ, USA

Introduction

While cancer has traditionally been associated with genetic damage, pharmacologic interventions for some forms of malignancies have recently focused on epigenetic damage. Epigenetic damage (i.e., the deactivation of genes after multiple cell divisions), which occurs due to factors such as aging and chronic inflammatory processes, has led to many treatment-resistant cancers such as myelodysplastic syndrome. DNA methylation is an important epigenetic marker; malignancy has been associated with hypomethylation of human tumor DNA as well as hypermethylation of tumor suppressor genes. Additionally, the acetylation of

Published online: 11 January 2012

core nucleosome histone proteins remodels chromatin, increases access to DNA of transcription factors and other co-activator proteins, and promotes gene transcription. Histone acetylation is accomplished by histone acetyl transferases (HATs), whereas the deacetylation of histones is accomplished by histone deacetylases (HDACs) [1]. In normal cells, HAT and HDAC activities are balanced and tightly regulated by homeostasis. However, excess HDAC activity is common in cancer cells and contributes to oncogenic transformation by mediating the function of oncogenic translocation products [2–4]. In patients with gastrointestinal (GI) malignancies, epigenetic deactivation of genes through DNA hypermethylation and histone deacetylation has been implicated, particularly in gastric cancer, in which patients are often affected by chronic gastritis due to *H. pylori* infection [5–7].

The activity of HDACs has been further elucidated recently to include modification of non-histone proteins such as transcription factors, tumor suppressor genes, cell cycle regulators, mediators of signal transduction, a cytoskeletal modifier, the molecular chaperone Hsp90, and SRY [8]. As a result, inhibition of HDACs was identified as a possible target for pharmacologic antineoplastic agents; clinical research with HDAC inhibitors has since validated these agents in a variety of solid tumor and hematologic malignancy settings [9–12].

There are 3 major classes of HDACs that include at least 18 isozymes; HDAC classes are separated based on size, cellular localization, number of catalytic active sites, and homology to yeast HDAC proteins. Class I HDACs are generally localized to the nucleus of cells and include HDAC1, HDAC2, HDAC3, and HDAC8 while class II HDACs shuttle between the nucleus and the cytoplasm and include two subclasses (Class IIa includes HDAC4, HDAC5, HDAC7, and HDAC9, each of which contains a single catalytic active site, and Class IIb includes HDAC6 and HDAC10, which both contain two active sites. Class III HDACs operate by a NAD^+-dependent mechanism unrelated to the other HDAC proteins.

Vorinostat (suberoylanilide hydroxamic acid) is a small molecule inhibitor of class I and II HDAC enzymes that has been shown to promote cell cycle arrest and apoptosis of cancer cells through regulation of gene expression [12, 13]. Vorinostat has demonstrated activity against various types of tumors in vitro and also improved survival and/or produced antitumor effects in animal models [9]. Interestingly, HDAC inhibitors, including vorinostat, reactivated RUNX3, a gastric tumor suppressor in gastric cancer-derived cells lines that is epigenetically silenced [14]. In addition, the loss of transforming growth factor-β (TGFβ) response contributes to oncogenesis and has been described in GI cancer [15, 16]. Vorinostat can restore TGFβ activity [17].

Vorinostat had a favorable toxicity profile in phase I and II trials in Japanese and non-Japanese patients [10, 11, 18–20]. Phase I trials to evaluate the safety and activity of vorinostat were conducted in patients with advanced solid and hematologic malignancies and demonstrated that oral vorinostat was well tolerated [18, 20]. Dose-limiting toxicities (DLTs) included anorexia, dehydration, diarrhea, fatigue, and thrombocytopenia. The maximum tolerated doses of oral vorinostat were determined to be 400 mg qd or 200 mg bid as continuous dosing, and 300 mg bid for 3 consecutive days per week, or 200 mg orally bid or tid for 14 days followed by 7 days of rest [18]. In two phase II trials, vorinostat 400 mg qd as continuous dosing was safe and effective, with an overall response rate of 24–30% in refractory advanced patients with cutaneous T-cell lymphoma (CTCL) including large cell transformation and Sézary syndrome [10, 19]. In October 2006, vorinostat was approved by the US Food and Drug Administration (FDA) for the treatment of cutaneous manifestations in patients with CTCL who have progressive, persistent or recurrent disease on or after two systemic therapies [21].

Based on these promising preclinical and clinical findings, a phase I trial of vorinostat in Japanese patients with solid tumors was conducted. In the study, vorinostat was generally well tolerated up to 500 mg daily for 14 days followed by 7 days of rest. The safety profile and pharmacokinetics data from Japanese patients were similar to those from non-Japanese patients [18, 22]. The current study was conducted in order to evaluate the safety, tolerability, and pharmacokinetics of two non-Japanese maximum tolerated doses (MTDs) of vorinostat (400 mg orally every day as continuous dosing, and 300 mg orally bid for 3 consecutive days per week) in Japanese patients; these dosing schedules were selected based on their dose intensities. An exploratory objective in this study was to determine if vorinostat has antitumor activity against GI cancer, especially gastric cancer.

Methods

This phase I study (Protocol 048) was conducted at 3 study centers in Japan and approved by Institutional Review Boards at each study center. All patients provided written informed consent prior to enrollment in accordance with principles of Good Clinical Practice. This study was conducted at the following sites: National Cancer Center Hospital East, Chiba, Japan; National Cancer Center, Tokyo, Japan; Oita University, Oita, Japan; Cancer Institute Hospital of the Japanese Foundation for Cancer Research, Oita, Japan; and Cancer Institute Hospital of the Japanese Foundation for Cancer Research, Tokyo, Japan.

Eligibility criteria

Patients who were eligible to enroll in this study included those with a histologically or cytologically diagnosed solid tumor with no standard therapy available or those who had failed to respond to standard therapy, with ECOG performance status of 0–2, whose life expectancy was ≥3 months after enrollment, and who were ≥20 years of age.

Patients were not eligible for enrollment if they had adverse events (AEs) from previous anti-cancer treatments that were National Cancer Institute Common Terminology Criteria for Adverse Events (CTCAE) version 3.0 grade 2 or more severe (with the exception of alopecia); were positive for HIV, HBV, or HCV; had a brain tumor or brain metastasis; had any concurrent malignancy (unless they had tumors localized in mucosa/epithelium or those who had been in remission for ≥5 years); had anemia requiring blood transfusions within 2 weeks before enrollment; had bone marrow, hepatic, or renal dysfunction beyond predefined criteria; had peritoneal or pleural effusion requiring treatment; or had any uncontrolled concomitant illness (arrhythmias, unstable angina, congestive heart failure, uncontrolled hypertension, infections requiring systemic treatment, or continuous use of steroids). Additionally, patients were excluded if they required immunotherapy, radiotherapy, surgery, or chemotherapy or if they underwent these procedures within 4 weeks before enrollment; had hematopoietic cytokine treatment (e.g., G-CSF) within 2 weeks before enrollment; had mitomycin C or nitrosoureas within 6 weeks before enrollment; had a history of radiotherapy directed toward >25% of hematopoietic marrow cells; or had previously participated in a clinical trial of an HDAC inhibitor. The use of prophylactic concomitant use of colony stimulating factors, antibiotics, or antiemetics was prohibited during the 1st cycle.

Treatment plan

The doses studied in this clinical trial were selected based on their dose intensities. A dose regimen of 200 mg bid for 14 days followed by 7 days of rest (a dose intensity of 5600 mg) had already been determined to be well tolerated in Japanese patients with solid tumors. Because this was the first study in Japanese patients with GI cancer treated with multiple prior chemotherapies, an initial dosing regimen of 300 mg bid for 3 consecutive days per week was chosen due to a lower dose intensity (5400 mg). The 400 mg qd dose was chosen for this study because it is the regimen recommended internationally for other cancers.

Treatment was administered at a hospital for the first cycle and at home for each subsequent cycle. Two dosing regimens that had been used in the previous clinical studies conducted outside Japan were investigated in this study: group 1 and group 2.

For group 1, vorinostat 300 mg (3 × 100-mg oral tablets) was administered twice daily for 3 consecutive days (within 30 min after breakfast and dinner) followed by 4 off-drug days; this was repeated 3 times for each cycle of treatment. For group 2, vorinostat 400 mg qd was administered for 21 consecutive days.

At least 3 evaluable patients for a dose-limiting toxicity (DLT) were enrolled in each dosing regimen using a standard "3 + 3" design. In order to assess the safety of each dosing regimen, we followed the procedure detailed in Fig. 1.

Additional patients were enrolled at the same level up to a total of 10 patients for each dosing regimen (a total of 20 patients) to evaluate pharmacokinetics once safety was confirmed. If a patient developed a DLT during a treatment cycle, the patient was to stop treatment for the rest of the days in the cycle, and the dose was reduced to 200 mg bid for 3 consecutive days followed by 4 off-drug days if the

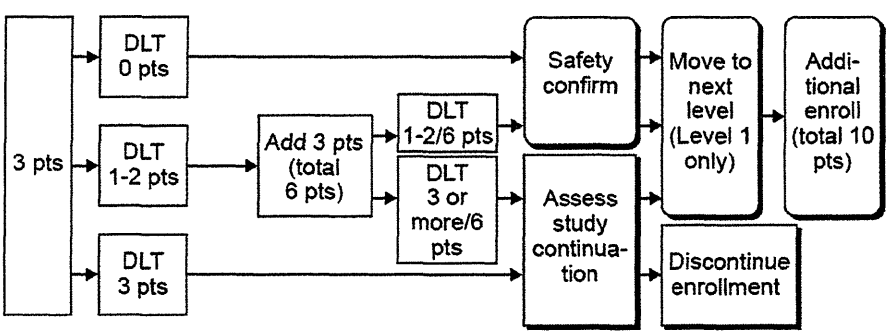

Fig. 1 Procedure for evaluating dose levels for safety based on DLTs: (1) If none of the first 3 patients at a level developed a DLT during the first cycle, the dose was deemed tolerable. (2) If 1 or 2 of the first 3 patients enrolled at a level developed a DLT during the first cycle, 3 additional patients were enrolled at the same level to further assess tolerability with 6 patients; if 2 or fewer of the 6 patients developed a DLT, the dose was deemed tolerable. If 3 or more of the 6 patients developed a DLT, continuation of the level was to be determined by the sponsor after assessment by the efficacy and safety board. (3) If all 3 patients enrolled at a level developed a DLT during the first cycle, continuation of the level was to be determined by the sponsor after assessment by the efficacy and safety board

patient was in group 1, or the dose was reduced to 300 mg qd for 21 consecutive days if the patient was in group 2 in the subsequent cycles.

Safety

Adverse experiences (AEs) were evaluated by investigators who determined their relationship to the study drug and degree of severity. The CTCAE version 3.0 was used to grade AEs. DLTs were defined as the manifestation of one of the following drug-related AEs: (1) grade 4 neutropenia persisting for more than 5 days; (2) grade 3 or higher neutropenia with fever; (3) grade 3 thrombocytopenia requiring platelet transfusions or grade 4 thrombocytopenia; (4) grade 3 or higher non-hematological toxicities; (5) AST/ALT elevation of over 300 IU/L.

Pharmacokinetics

Serum vorinostat concentration was analyzed using a turbulent flow on-line extraction format for analyte isolation followed by reversed-phase high-performance liquid chromatography with tandem mass spectrometric detection. Pharmacokinetic parameters (AUC, C_{max}, T_{max} and $t_{1/2}$) were calculated according to a noncompartmental analysis from the serum concentration of vorinostat based on actual blood sampling time pre-dose and post-dose (at 0.25, 0.5, 1, 1.5, 2, 3, 4, 6, 8, 10, 12, and 24 h after administration of vorinostat) on Day 1, Day 3 of the 1st cycle at dose level 1 and Day 1, Day 21 of the 1st cycle at dose level 2. WinNonLin Professional version 5.0.1 (Pharsight Corp., Mountain View, CA, USA) was used for the pharmacokinetic analysis.

Efficacy

Tumor response was assessed according to the RECIST Version 1.0 guidelines [23] in patients with evaluable lesions. Tumor markers were chosen by investigators based on the type of cancer. All assessments required at baseline were performed within 4 weeks of the initiation of the study treatment. After initiation of treatment, tumor response was assessed by imaging at least every 6 weeks (every 2 cycles).

Target lesions were set by choosing up to 5 measurable lesions in one organ and up to 10 measurable lesions in the whole body. Tumor response was assessed by using the following criteria: complete response (CR) was assigned when all target lesions disappeared for 4 weeks; partial response (PR) was assigned when the sum of the longest diameters of the target lesions were reduced by ≥30% for 4 weeks; progressive disease (PD) was assigned when the sum of the longest diameters of the target lesions increased by ≥20% from the minimum sum recorded during treatment; and stable disease (SD) was assigned when the change in tumor size was not sufficient to assign PR or PD. For non-target lesions, CR was assigned when all non-target lesions disappeared or levels of all tumor markers had been normalized; incomplete response (IR) or SD was assigned when one or more non-target lesion persisted or levels of one or more tumor markers were higher than the upper limit of normal; PD was assigned for non-target tumors when there was an apparent aggravation of pre-existing non-target lesions. New lesions were recorded and treated as non-target lesions. An evaluation of overall response was also conducted by evaluating the response to target lesions, non-target lesions, and presence of new lesions.

Statistical methods

The primary purpose of the present study was to confirm safety. Therefore, the sample size was dependent on the occurrence of DLTs, although 20 patients were to be enrolled in order to obtain pharmacokinetics data. Because data were insufficient for the purpose of estimating the width of confidence intervals, there was no power calculation. A significance level of 5% (two-tailed) was used for all analyses. No adjustments were made for multiplicity since the primary objective of the study was to confirm safety.

For the evaluation of safety, the incidence of patients with AEs, drug-related AEs, and DLTs were summarized by dose levels and grades. For laboratory test parameters, vital sign parameters, and body weight, summary statistics (mean, standard error, minimum, and maximum) were provided. For the 12-lead ECG, a table of the number and percent of patients experiencing abnormalities was summarized by dose levels and time points.

For pharmacokinetic analysis, summary statistics of each pharmacokinetic parameter (AUC, C_{max}, T_{max} and $t_{1/2}$) were calculated. For calculation of AUC and C_{max}, logarithmic transformed values were used. To assess the effect of a repeated administration on pharmacokinetic parameters, the geometric mean ratio of $AUC_{0-12\ h}$ (Day 3/Day 1) and its 90% confidence interval at dose level 1 was calculated. On dose level 2, only the geometric mean ratio of $AUC_{0-24\ h}$ (Day 21/Day 1) was calculated because of limited available data ($n = 2$). For Day 8 at dose level 2, summary statistics were calculated as the trough value of serum concentration of vorinostat. For the other pharmacokinetic parameters, the appropriate transformation was done.

The exploratory analysis of efficacy was performed by summarizing the response of each dosing regimens using RECIST Version 1.0 guidelines.

Results

Patient characteristics

A total of 16 patients were enrolled in this study; 10 at dose level 1 (group 1) and 6 at dose level 2 (group 2). Baseline patient characteristics are shown in Table 1. The specific diagnoses for the patients who enrolled in this study included gastric cancer, colon cancer, and rectal cancer. The median numbers of prior regimens were 3.5 (range 2–6) for patients in group 1 and 4.5 (range 3–6) for those in group 2.

Table 1 Baseline characteristics

	300 mg bid × 3 days/ week (n = 10)	400 mg qd 21 consecutive days (n = 6)
Median age, years [range]	61 [43–73]	55 [32–66]
Male (n)	8	4
Female (n)	2	2
ECOG performance status (n)		
0	9	2
1	1	4
Disease type (n)		
Gastric cancer	8	2
Colon cancer	1	1
Rectal cancer	1	3
Number of prior chemotherapy regimens [range]	3.5 [2–6]	4.5 [3–6]

Safety and tolerability

Group 1 (300 mg bid for 3 consecutive days followed by 4 rest days)

There were 10 patients who received vorinostat in group 1. The median treatment duration was 52.0 days (range 17–243). In this group of patients, no DLTs were observed. The most common drug-related AEs included anorexia, nausea, and fatigue (Table 2). Of these drug-related AEs, the instances of thrombocytopenia were considered grade 3/4.

Four patients in group 1 experienced serious AEs. Of these, abdominal pain (grade 2) and diarrhea (grade 2), and vomiting (grade 2) and abdominal pain (grade 1) were considered by the investigator to be drug-related. Since these events required hospitalization for a follow-up, they corresponded to serious AEs. Disease progression and hyperbilirubinaemia were considered to be unrelated to the study drug.

One death was reported during this study. The patient, who had a primary disease of gastric cancer, showed disease progression at the end of the first cycle and completed the study. The patient died 26 days after the end of study therapy. The death was considered to be due to underlying disease progression and not related to the study drug.

Group 2 (400 mg qd for 21 consecutive days)

There were 6 patients who received vorinostat in group 2. The median treatment duration was 51.5 days. Of these 6 patients, 2 patients did not complete the first cycle and were not included in the DLT assessment. Of the 4 remaining patients, 2 patients developed DLTs of grade 4 thrombocytopenia. The two patients in group 2 had dose reductions from 400 mg qd to 300 mg qd. The most

Table 2 Most common drug-related hematologic and non-hematologic AEs

	Total (n = 16)		300 mg bid × 3 days/ week (n = 10)		400 mg qd 21 consecutive days (n = 6)	
	Grade 1 or 2	Grade 3 or 4	Grade 1 or 2	Grade 3 or 4	Grade 1 or 2	Grade 3 or 4
Hematologic						
Thrombocytopenia	4	5	2	1	2	4
Lymphopenia	7	0	4	0	3	0
Non-hematologic						
Anorexia	15	0	9	0	6	0
Nausea	14	0	8	0	6	0
Fatigue	11	0	8	0	3	0
Hyperglycemia	11	0	6	0	5	0
Vomiting	9	0	5	0	4	0
Blood creatinine increased	9[a]	0	4	0	4	0

[a] One patient experienced blood creatinine increase after dose reduction from 400 mg qd to 300 mg qd

common drug-related AEs included anorexia, nausea and thrombocytopenia (Table 2). There were 4 cases of thrombocytopenia that were considered to be grade 3/4 in group 2.

One patient in group 2 discontinued due to AEs. The patient experienced acetonemic vomiting and gastric hemorrhage due to primary disease.

Pharmacokinetics

In group 1, the maximum serum concentrations (C_{max}) of vorinostat were observed at 0.50–5.97 h after the first dose on Day 1 and 0.25–6.00 h after the morning dose on Day 3 following 3 days of multiple oral doses of vorinostat 600 mg daily (300 mg × 2) with food. Vorinostat was then rapidly eliminated with apparent $t_{1/2}$ of 0.94–1.05 h on average. The $AUC_{0-12\ h}$ was 3.92 ± 1.52 μM h after the first dose on Day 1 and 4.19 ± 1.84 μM h after the morning dose on Day 3. C_{max} was 1.17 ± 0.43 μM h after the first dose on Day 1 and 1.32 ± 0.75 μM h after the morning dose on Day 3. These results suggest that there was no significant change in absorption or elimination of vorinostat. The accumulation ratio of vorinostat following 3 days of multiple oral dose was 1.07 (90% confidence interval; 097, 1.18), suggesting no accumulation after administration of vorinostat with this dose regimen (Table 3).

In group 2, the C_{max} were observed by 3.80–6.00 h after the first dose and 2.98–3.67 h after the final dose. Vorinostat was eliminated rapidly with an apparent $t_{1/2}$ of 1.17–1.49 h on average. The $AUC_{0-24\ h}$ was 7.97 ± 3.05 μM h after the first dose and 8.45 μM h after the final dose. C_{max} was 1.62 ± 0.52 μM h after the first dose and 2.04 μM h after the final dose. At this dosing level, we were unable to evaluate the effect of multiple dosing on the pharmacokinetic parameters because the parameters following the final dose were calculated for only 2 patients. In these 2 patients, the accumulation ratio was 1.50, but because of limited data, these results should be viewed with caution (Table 4).

Patients with higher AUC values had more AEs compared with those who had lower AUC values. The other studies show the similar result of the correlation between AUC and AEs.

Efficacy

In group 1, of the 10 patients who received vorinostat, 5 patients achieved stable disease ≥8 weeks as best response: 4 patients with gastric cancer, 1 patient with colon cancer. Of these, one patient with gastric cancer showed sustained stable disease for up to 245 days. The median duration of time to progression (TTP) was 70 days (range 21–245 days).

In group 2, of the 6 patients who received vorinostat, 3 patients achieved stable disease as best response. Of these, 2 patients achieved stable disease ≥8 weeks: 1 patient with colon cancer and 1 patient with rectosigmoid cancer; no patients in group 2 with the specific diagnosis of gastric cancer had SD or better (Fig. 2).

Table 3 Summary of serum pharmacokinetic parameters at 300 mg bid × 3 days/week

Parameter	Day 1 (n = 10, fed state)	Day 3 (n = 10, fed state)
$AUC_{0-\infty}$ (μM h)	3.94 ± 1.56	4.15 ± 2.15[a]
$AUC_{0-12\ h}$ (μM h)	3.92 ± 1.52	4.19 ± 1.84
C_{max} (μM)	1.17 ± 0.43	1.32 ± 0.75
T_{max} (h)	1.99 (0.50–5.97)	0.99 (0.25–6.00)
$t_{1/2}$ (h)	1.05 ± 0.32	0.94 ± 0.54[a]
Accumulation ratio[b]	–	1.07 (0.97, 1.18)

$AUC_{0-\infty}$, area under the concentration time curve from zero to infinity; $AUC_{0-12\ h}$, AUC from time to zero to 12 h; C_{max}, maximum concentration; $t_{1/2}$, terminal half life; $AUC_{0-\infty}$, $AUC_{0-12\ h}$ and C_{max}, geometric mean ± geometric SD; T_{max}, median (range); $t_{1/2}$, harmonic mean ± Jackknife SD

[a] n = 9 (Since the terminal elimination phase was not able to be evaluated in one patient, the $t_{1/2}$ and $AUC_{0-\infty}$ could not be determined.)

[b] $AUC_{0-12\ h,\ Day\ 3}/AUC_{0-12\ h,\ Day\ 1}$ (geometric mean)

Table 4 Summary of serum pharmacokinetic parameters at 400 mg qd for 21 consecutive days

Parameter	Day 1 (n = 5[a], fed state)	Day 21 (n = 2[b], fed state)
$AUC_{0-\infty}$ (μM h)	7.75 ± 2.79	8.30
$AUC_{0-24\ h}$ (μM h)	7.97 ± 3.05	8.45
C_{max} (μM)	1.62 ± 0.52	2.04
T_{max} (h)	3.93 (3.80–6.00)	3.33 (2.98–3.67)
$t_{1/2}$ (h)	1.49 ± 0.82	1.17
Accumulation ratio[c]	–	1.50

$AUC_{0-\infty}$, area under the concentration time curve from zero to infinity; $AUC_{0-24\ h}$, AUC from time to zero to 24 h; C_{max}, maximum concentration; $t_{1/2}$, terminal half life; $AUC_{0-\infty}$, $AUC_{0-24\ h}$ and C_{max}, geometric mean ± geometric SD; T_{max} median (range); $t_{1/2}$, harmonic mean ± Jackknife SD, accumulation ratio:geometric mean

[a] Serum pharmacokinetic parameters on Day 1 in one patient were unavailable for calculation of mean and SD because the subject vomited after administration on Day 1

[b] Mean serum pharmacokinetic parameters on Day 21 were calculated from 2 patients

[c] $AUC_{0-24\ h,\ Day\ 21}/AUC_{0-24\ h,\ Day\ 1}$ (geometric mean)

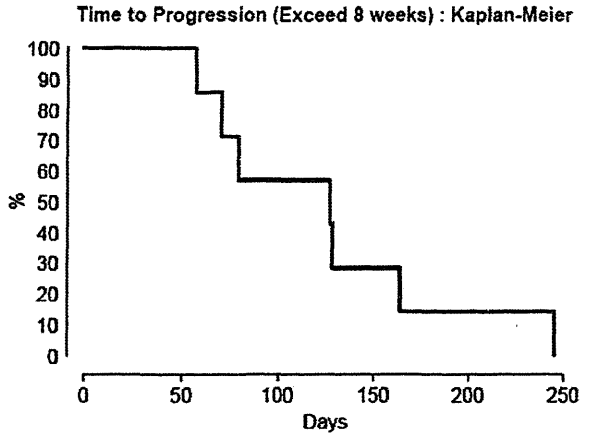

Type of Cancer	Number of Prior Chemotherapy Regimens	Best Response	Time to Progression (days)
300 b.i.d × 3 days/week			
Rectal cancer	3	SD	127
Gastric cancer	2	SD	164
Gastric cancer	6	SD	70
Gastric cancer	2	SD	245
Gastric cancer	4	SD	128
400 q.d.			
Rectosigmoid cancer	6	SD	79
Colon cancer	3	SD	57

Fig. 2 Patients who achieved stable disease lasting ≥8 weeks (56 days)

Discussion

Previous studies, conducted in Japanese and non-Japanese populations, have evaluated vorinostat in a variety of conditions, including hematologic and solid malignancies, with various dosing regimens [10, 11, 18–20]. The results of the present study demonstrated that vorinostat was generally well tolerated. The most common drug-related AEs were anorexia, nausea, fatigue, and hyperglycemia; these AEs occurred in both dosing regimens and have been observed in previous vorinostat studies [10, 11, 18–20]. These drug-related AEs were grade 1/2. In patients who experienced DLTs, pharmacokinetic exposure was relatively higher; patients with higher AUC values also had more AEs compared with those who had lower AUC values in other studies.

In the treatment of CTCL, the dosing regimen approved by the United States FDA is 400 mg qd as continuous dosing [10, 19, 21]. It should be noted that CTCL differs from solid cancers such as the gastric cancer treated in the present study. In general, prior therapies in patients with CTCL include topical treatments such as interferon-γ and bexarotene or systemic treatments such as monoclonal antibodies, immune response modifiers (IFNs and retinoids), and well-tolerated antiproliferative drugs such as methotrexate [24], whereas combination chemotherapy is the standard therapy for patients with gastric and colorectal cancer [25].

Given the greater number and different types of prior therapies in patients with gastric and colorectal cancer, it is likely that the tolerability results observed in this study would reflect the heavily pretreated nature of this patient population. Indeed, with regard to DLTs and grade 3/4 AEs, it was apparent that the 300 mg bid dose for 3 consecutive days followed by 4 days of rest [a dose associated with a lower dose intensity (5400 mg per cycle) compared with 400 mg qd (6300 mg per cycle)] resulted in greater tolerability compared with the 400 mg qd dose. Additionally of note, because of the platelet-suppressing effects of vorinostat, hematologic effects, such as thrombocytopenia, are expected with vorinostat use. With regard to hematologic toxicities, there was an apparent advantage to the 300 mg bid dosing regimen; grade 3/4 thrombocytopenia AEs were observed in 4 out of 6 patients who received 400 mg qd for 21 consecutive days compared with only 1 out of 10 patients who received 300 mg bid for 3 consecutive days followed by 4 days of rest.

Another Phase I study recently assessed the safety and pharmacokinetics of vorinostat 100 mg bid, 200 mg bid, 400 mg qd, and 500 mg qd in 18 Japanese patients with solid tumors (roughly half of the patients had non-small cell lung cancer; the rest had bile duct cancer, invasive thymoma, esophageal cancer, and malignant mesothelioma) [20]. The results of that study were similar to those observed in the present study in terms of the types of AEs that patients experienced (thrombocytopenia, anorexia, and fatigue). However, the 400 and 500 mg qd doses in that study were better tolerated compared with the 400 mg qd dose in the present study. The mean drug exposure observed in that study was comparable to that observed in the current study for the 300 mg bid dose level, but lower than the 400 mg qd dose level in the present study [20]. Of note, the number of prior chemotherapy regimens among patients in the present study was higher compared with the number of prior chemotherapy regimens among patients in the Fujiwara et al. [20] study, again highlighting the possibility that tolerability may be affected by the nature of prior therapies. On the other hand, the serum exposure of the 400 mg qd dose level in the present study was higher than those of the 400 and 500 mg doses in that study. Identification of the reason is difficult due to the small number of enrolled patients. Also, the relationship between change in pharmacokinetics with vorinostat and the following factors cannot be demonstrated because of variation in concomitant therapy as well as the small number of enrolled patients. However, potential factors could include differences in health status of patients enrolled in the study and/or concomitant therapy during dosing with vorinostat.

These may affect physiology (for example, migration rate in GI tract, epithelial cells in GI tract, blood flow rate, etc.), and produce large inter-individual variability in vorinostat pharmacokinetics. Therefore, there is a possibility that the high serum exposures observed in some of the enrolled patients were due to such multiple factors. Patients with metastatic disease were not examined in this trial and the evidence for the effect of vorinostat in patients with metastatic disease is scant. In small studies in patients with metastatic breast cancer, head and neck cancer, and thyroid carcinoma, stand-alone vorinostat was generally well tolerated but led to neither complete nor partial response in any patient, although the stable disease achieved by some patients warrants further research in combination therapy [26–28].

Although efficacy in the treatment of gastric cancer was not a primary objective for this study, 5 patients in group 1 (300 mg bid) achieved stable disease $\geq$8 weeks, with 1 patient in particular having duration of TTP of 245 days. In contrast, there were two patients in group 2 (400 mg qd) who achieved stable disease $\geq$8 weeks, possibly due to the lower tolerability observed with this dosing regimen. We observed these results despite the fact that 300 mg bid resulted in lower mean drug exposure compared with 400 mg qd, indicating that the lower drug exposure associated with the 300 mg bid dose level led to greater tolerability with no deleterious effects on efficacy compared with the higher observed drug exposure at the 400 mg qd dose level. Objective responses were not observed in this study. However, considering the cytostatic effect of vorinostat in preclinical models, these data appear to be encouraging [9, 29]. In a previous phase I study in non-Japanese patients, the administration of vorinostat with 300 mg or 400 mg bid for 3 consecutive days followed by 4 days rest regimen showed PR in 2 patients, and stable disease $\geq$16 weeks in 3 patients out of 13 patients with malignant pleural mesothelioma [30]. Therefore, from a safety and efficacy perspective, this dosing regimen is promising for Japanese patients with GI cancer. Currently, a phase III study is on-going to evaluate 300 mg bid for 3 consecutive days followed by 4 days rest in non-Japanese and Japanese patients with mesothelioma.

When viewing these data, the limitations of the current study should be considered. Specifically, the results from this study are limited due to the small number of patients studied, and further investigation is needed to assess tolerability in a larger patient population. More research is also needed to further characterize the efficacy of vorinostat with regard to whether or not efficacy is dose-dependent and whether differentiated gastric cancer is more responsive to treatment than undifferentiated gastric cancer.

In conclusion, vorinostat given to patients with GI cancer was well tolerated when given 300 mg bid for 3 consecutive days followed by 4 days of rest when compared with 400 mg qd dosing regimen for 21 consecutive days per cycle in Japanese patients. Additionally, 5 patients receiving 300 mg bid and 2 patients receiving 400 mg qd maintained stable disease for >8 weeks, with the maximum duration being 245 days. The current study supports further investigation of vorinostat alone or in combination with other anti-cancer agents in patients with gastric cancer who may be sensitive to epigenetic treatment with an HDAC inhibitor, such as those who exhibit aberrant DNA methylation of p16. Of particular interest will be the evaluation of overlapping hematologic toxicities for the study of a combination approach with other agents with low rates of toxicities. For further study of vorinostat alone, the rate of efficacy will need to be evaluated in a larger population of patients to ensure adequate treatment of gastric cancer.

Conflict of interest Noguchi and Otsuki are employees of MSD K.K., a subsidiary of Merck & Co., Inc., and may own stock or stock options in the company. Mehta is an employee of Merck Sharp & Dohme, Corp., and may own stock or stock options in the company. The other authors report no conflicts of interest.

References

1. Minucci S, Pelicci PG (2006) Histone deacetylase inhibitors and the promise of epigenetic (and more) treatments for cancer. Nat Rev Cancer 6:38–51
2. Marks P, Rifkind RA, Richon VM et al (2001) Histone deacetylases and cancer: causes and therapies. Nat Rev Cancer 1:194–202
3. Timmermann S, Lehrmann H, Polesskaya A et al (2001) Histone acetylation and disease. Cell Mol Life Sci 58:728–736
4. Wang C, Fu M, Mani S et al (2001) Histone acetylation and the cell-cycle in cancer. Front Biosci 6:D610–29, D610–29
5. Ueno M, Toyota M, Akino K et al (2004) Aberrant methylation and histone deacetylation associated with silencing of SLC5A8 in gastric cancer. Tumour Biol 25:134–140
6. Murai M, Toyota M, Suzuki H et al (2005) Aberrant methylation and silencing of the BNIP3 gene in colorectal and gastric cancer. Clin Cancer Res 11:1021–1027
7. Kawamura YI, Toyota M, Kawashima R et al (2008) DNA hypermethylation contributes to incomplete synthesis of carbohydrate determinants in gastrointestinal cancer. Gastroenterology 135:142–151
8. Marson CM (2009) Histone deacetylase inhibitors: design, structure-activity relationships and therapeutic implications for cancer. Anticancer Agents Med Chem 9:661–692
9. Butler LM, Agus DB, Scher HI et al (2000) Suberoylanilide hydroxamic acid, an inhibitor of histone deacetylase, suppresses the growth of prostate cancer cells in vitro and in vivo. Cancer Res 60:5165–5170
10. Duvic M, Talpur R, Ni X et al (2007) Phase 2 trial of oral vorinostat (suberoylanilide hydroxamic acid, SAHA) for refractory cutaneous T-cell lymphoma (CTCL). Blood 109:31–39
11. Galanis E, Jaeckle KA, Maurer MJ et al (2009) Phase II trial of vorinostat in recurrent glioblastoma multiforme: a north central cancer treatment group study. J Clin Oncol 27:2052–2058
12. Secrist JP, Zhou X, Richon VM (2003) HDAC inhibitors for the treatment of cancer. Curr Opin Investig Drugs 4:1422–1427

13. Richon VM, Garcia-Vargas J, Hardwick JS (2009) Development of vorinostat: current applications and future perspectives for cancer therapy. Cancer Lett 280:201–210
14. Huang C, Ida H, Ito K et al (2007) Contribution of reactivated *RUNX3 to inhibition of gastric cancer cell growth following* suberoylanilide hydroxamic acid (vorinostat) treatment. Biochem Pharmacol 73:990–1000
15. Gordon KJ, Blobe GC (2008) Role of transforming growth factor-beta superfamily signaling pathways in human disease. Biochim Biophys Acta 1782:197–228
16. Bierie B, Moses HL (2006) Tumour microenvironment: TGFbeta: the molecular Jekyll and Hyde of cancer. Nat Rev Cancer 6:506–520
17. Ammanamanchi S, Brattain MG (2004) Restoration of transforming growth factor-beta signaling through receptor RI induction by histone deacetylase activity inhibition in breast cancer cells. J Biol Chem 279:32620–32625
18. Kelly WK, O'Connor OA, Krug LM et al (2005) Phase I study of an oral histone deacetylase inhibitor, suberoylanilide hydroxamic acid, in patients with advanced cancer. J Clin Oncol 23:3923–3931
19. Olsen EA, Kim YH, Kuzel TM et al (2007) Phase IIb multicenter trial of vorinostat in patients with persistent, progressive, or treatment refractory cutaneous T-cell lymphoma. J Clin Oncol 25:3109–3115
20. Fujiwara Y, Yamamoto N, Yamada Y et al (2009) Phase I and pharmacokinetic study of vorinostat (suberoylanilide hydroxamic acid) in Japanese patients with solid tumors. Cancer Sci 100:1728–1734
21. Mann BS, Johnson JR, Cohen MH, Justice R et al (2007) FDA approval summary: vorinostat for treatment of advanced primary cutaneous T-cell lymphoma. Oncologist 12:1247–1252
22. Rubin E, Agrawal N, Friedman E et al (2006) A study to determine the effects of food and multiple dosing on the pharmacokinetics of vorinostat given orally to patients with advanced cancer. Clin Cancer Res 12:7039 doi:10.1158/1078-0432.CCR-06-1802
23. Gehan EA, Tefft MC (2000) Will there be resistance to the RECIST (response evaluation criteria in solid tumors)? J Natl Cancer Inst 92:179–181
24. Dummer R, Cozzio A, Meier S et al (2006) Standard and experimental therapy in cutaneous T-cell lymphomas. J Cutan Pathol 33(Suppl 1):52–57
25. Nishiyama M, Eguchi H (2009) Pharmacokinetics and pharmacogenomics in gastric cancer chemotherapy. Adv Drug Deliv Rev 61:402–407
26. Luu TH, Morgan RJ, Leong L et al (2008) A phase II trial of vorinostat (suberoylanilide hydroxamic acid) in metastatic breast cancer: a california cancer consortium study. Clin Cancer Res 14:7138–7142
27. Woyach JA, Kloos RT, Ringel MD et al (2009) Lack of therapeutic effect of the histone deacetylase inhibitor vorinostat in patients with metastatic radioiodine-refractory thyroid carcinoma. J Clin Endocrinol Metab 94:164–170
28. Blumenschein GR, Jr, Kies MS, Papadimitrakopoulou VA et al (2008) Phase II trial of the histone deacetylase inhibitor vorinostat (Zolinza, suberoylanilide hydroxamic acid, SAHA) in patients with recurrent and/or metastatic head and neck cancer. Invest New Drugs 26:81–87
29. Lobjois V, Frongia C, Jozan S et al (2009) Cell cycle and apoptotic effects of SAHA are regulated by the cellular microenvironment in HCT116 multicellular tumour spheroids. Eur J Cancer 45:2402–2411
30. Krug LM, Curley T, Schwartz L et al (2006) Potential role of histone deacetylase inhibitors in mesothelioma: clinical experience with suberoylanilide hydroxamic acid. Clin Lung Cancer 7:257–261

European Journal of Pharmacology 689 (2012) 72–80

Contents lists available at SciVerse ScienceDirect

European Journal of Pharmacology

journal homepage: www.elsevier.com/locate/ejphar

Neuropharmacology and analgesia

Zonisamide up-regulated the mRNAs encoding astrocytic anti-oxidative and neurotrophic factors

Choudhury ME[a], Sugimoto K[b], Kubo M[a], Iwaki H[a], Tsujii T[a], Kyaw WT[a], Nishikawa N[a], Nagai M[a], Tanaka J[b], Nomoto M[a,c,*]

[a] Department of Therapeutic Medicine (Clinical Pharmacology and Neurology), Ehime University Graduate School of Medicine, Shitsukawa, Toon-Shi, Ehime 791-0295, Japan
[b] Department of Basic and Clinical Neuroscience, Ehime Proteo-Medicine Research Center, Ehime University, Shitsukawa, Toon-Shi, Ehime 791-0295, Japan
[c] Phase 1 Unit, Therapeutic Research Center, Ehime University Hospital, Shitsukawa, Toon-Shi, Ehime 791-0295, Japan

ARTICLE INFO

Article history:
Received 13 February 2012
Received in revised form
27 April 2012
Accepted 15 May 2012
Available online 31 May 2012

Keywords:
Zonisamide
Dopamine neuron
Astrocyte
Slice culture
6-Hydroxydopamine
(Rat)

ABSTRACT

Zonisamide has been proven as an effective drug for the recovery of degenerating dopaminergic neurons in the animal models of Parkinson's disease. However, several lines of evidence have questioned the neuroprotective capacity of zonisamide in animal models of Parkinson's disease. Although it suppresses dopaminergic neurodegeneration in animal models, the cellular and molecular mechanisms underlying the effectiveness of zonisamide are not fully understood. The current study demonstrates the effects of zonisamide on astrocyte cultures and two 6-hydroxydopamine-induced models of Parkinson's disease. Using primary astrocyte cultures, we showed that zonisamide up-regulated the expression of mRNA encoding mesencephalic astrocyte-derived neurotrophic factor, vascular endothelial growth factor, proliferating cell nuclear antigen, metallothionein-2, copper/zinc superoxide dismutase, and manganese superoxide dismutase. Similar responses to zonisamide were found in substantia nigra where the rats were pre-treated with 6-hydroxydopamine. Notably, pharmacological inhibition of 6-hydroxydopamine-induced toxicity by zonisamide pre-treatment was also confirmed using rat mesencephalic organotypic slice cultures of substantia nigra. In addition to this, zonisamide post-treatment also attenuated the nigral tyrosine hydroxylase-positive neuronal loss induced by 6-hydroxydopamine. Taken together, these studies demonstrate that zonisamide protected dopamine neurons in two Parkinson's disease models through a novel mechanism, namely increasing the expression of some important astrocyte-mediated neurotrophic and anti-oxidative factors.

1. Introduction

Zonisamide (1, 2-benzisoxazole-3-methanesulfonamide) is approved as an anti-parkinsonian drug by the Pharmaceuticals and Medical Devices Agency, Japan, as an adjunctive therapy for the patients with Parkinson's disease. A double-blind, controlled study has reported that the adjunctive zonisamide treatment with levodopa can improve the motor fluctuation, akinesia, and tremor of Parkinson's disease (Murata et al., 2007). Zonisamide is also effective in managing impulse control disorders in the patients with Parkinson's disease (Bermejo et al., 2010). Furthermore, intractable resting and re-emergent tremor in the patients with Parkinson's disease is improved dramatically by zonisamide (Iijima et al., 2011).

Mechanistically, zonisamide is an monoamine oxidase B inhibitor, as reported by its activity against 1-methyl-4-phenyl-1,2,3,6-tetrahydropyridine (MPTP)-induced toxicity (Sonsalla et al., 2010). Zonisamide is also effective in lessening the neurotoxicity of dopamine quinones which cause dopaminergic neuron-specific oxidative stress (Asanuma et al., 2008) and it has shown selective neuroprotection against complex I mitochondrial dysfunction (Costa et al., 2010). The protective effects of zonisamide against MPTP-induced neurotoxicity have been proven in mice and marmosets where it increases tyrosine hydroxylase protein in the dopaminergic system (Choudhury et al., 2010; Yano et al., 2009). Zonisamide has also been shown to suppress the 6-hydroxydopamine-induced endoplasmic reticulum stress of dopamine neurons by increasing ubiquitin ligase HRD1 protein and by suppressing caspase-3 activation (Omura et al., 2011). In a recent study by our group (Choudhury et al., 2011a), it was suggested that zonisamide protects dopamine neurons via astrocyte-derived S100β and the prolongation of this astrocyte-mediated process improved the recovery of MPTP-treated dopamine neurons.

* Corresponding author at: Department of Therapeutic Medicine, Ehime University Graduate School of Medicine, Shitsukawa, Toon-shi, Ehime 791-0295, Japan. Tel.: +81 89 960 5095; fax: +81 89 960 5938.
E-mail address: nomoto@m.ehime-u.ac.jp (M. Nomoto).

0014-2999/$ - see front matter © 2012 Elsevier B.V. All rights reserved.
http://dx.doi.org/10.1016/j.ejphar.2012.05.012

To obtain more insight into the pharmacological basis of the activity of zonisamide, we conducted two *in vitro* studies using cultures of rat primary astrocytes and 6-hydroxydopamine-treated organotypic midbrain slices. The *in vitro* results of these current studies are in good accordance with those obtained *in vivo*, and suggest that zonisamide elicits its protective actions on dopaminergic neurons, at least partly, by modulating the functions of astrocytes.

2. Materials and methods

2.1. Chemicals

Zonisamide and its sodium salt were kindly provided by Dainippon Sumitomo Pharma (Osaka, Japan). 6-Hydroxydopamine hydrobromide and N-methyl-D-aspartic acid were purchased from Sigma (St. Louis, MO, USA).

2.2. Animals

Wistar rats were housed under standard laboratory conditions and allowed free access to food and water throughout the experiments. The rats were kept in a 12/12 h dark/light cycle. The use of the animals was in strict accordance with the principles for animal experimentation at Ehime University Graduate School of Medicine. All efforts were made to minimize animal suffering and to reduce the number of animals used. The animals were humanely euthanized and the skulls were removed to expose the brains.

2.3. Preparation of primary astrocyte cultures

Primary cultures of rat astrocytes were prepared as previously described (Tanaka et al., 1998). Briefly, whole forebrains from neonatal rats were dissected out and dissociated into individual cells using a nylon bag with 160-μm pores. The dissociated cells as a mixed glial cell culture were cultured in 75-cm^2 flasks with 10% fetal calf serum-supplemented in Dulbecco's modified Eagle's medium (DMEM). On the 10th day of culturing, the culture flasks were vigorously shaken for 2 h to remove microglial cells and cells belonging to the O-2A lineage. On the 12th day of culturing, the flasks were again shaken vigorously for 4 h and cells attached to the flasks were treated with trypsin-EDTA solution (Sigma Chemical Co.). The detached cells were re-seeded on poly-L-lysine-coated 24-well plates or on glass cover slips in 4-well plates at a density of 2.5×10^4 cells/cm^2. The astroglial culture dishes were divided into five groups and treated with zonisamide (as mentioned briefly in Supplementary material, Table 1A). Astrocytes cultures were then processed by quantitative real-time polymerase chain reaction (qRT-PCR).

2.4. Construction of organotypic slice cultures

Slice cultures were prepared from 7-day-old post-natal rats as described elsewhere (Kress and Reynolds, 2005) with slight modification. Briefly, brains were harvested in a clean bench chamber and 4-mm thick blocks were prepared from the posterior hypothalamus to the anterior pons using a chilled metal slicer (Paxinos and Watson, 2009). Blocks were attached to a vibratome stage using instant glue and these were placed into a vibratome (Leica VT 1200S, Germany) with immersion in chilled phosphate-buffered saline (PBS) containing streptomycin and penicillin. Coronal slices (400-μm thicken) were taken and collected into 12-well plates filled with chilled DMEM. Two slices per animal were selected for our organotypic slice culture study (Paxinos and Watson, 2009). Slices were then immediately transferred to 12-well plates, soaked in E2-medium [serum-free DMEM containing 10 mM HEPES pH 7.3 (Invitrogen, Carlsbad, CA, USA), 4.5 mg/ml glucose, 5 μg/ml insulin, 5 nM sodium selenite, 5 μg/ml transferrin (Roche Diagnostic Japan, Tokyo, Japan), and 0.2 mg/ml bovine serum albumin (Sigma Chemical Co.)], and incubated in a CO_2 incubator for 10 day. Finally, after the slices had been incubated with zonisamide for 24 h, they were exposed to the neurotoxins 6-hydroxydopamine (100 μM) and N-methyl-D-aspartic acid (50 μM) for 48 h. The simultaneous use of 6-hydroxydopamine and N-methyl-D-aspartic acid effectively induced dopaminergic neurodegeneration, as described elsewhere (Kress and Reynolds, 2005). Finally, the slices were processed for immunoblotting study.

2.5. Construction of the animal model for Parkinson's disease

Male rats of 70 ± 1 day old were treated with 6-hydroxydopamine as previously described (Choudhury et al., 2011b) with minor changes. Briefly, the animals were maintained under pentobarbital sodium anesthesia (63 mg/kg) and placed in a stereotactic instrument (Narishige, Tokyo, Japan). 6-Hydroxydopamine was dissolved in saline containing ascorbic acid (Wako Pure Chemical Industries, Ltd., Osaka, Japan) [10 μg/μl dissolved in 1% ascorbate-saline]. The rats were then given unilateral injections of 6-hydroxydopamine. For unilateral injection, 5 μl of 6-hydroxydopamine was drawn into a Hamilton syringe and then injected into the right side of the striatum through a drilled hole in the skull at 1 mm anterior to the bregma and 3 mm lateral from the midline. The depth of the needle tip was 5 mm from the skull surface. The rate of fluid injection was 1 μl/min, which was maintained by pushing in 0.25 μl fluid every 15 s. The needle was left at the injection site for an additional 10 min after the injection and then slowly withdrawn. During recovery, rats received electrolyte solution (Solita-T3, Ajinomoto Pharmaceuticals, Tokyo, Japan). Zonisamide was dissolved in normal saline with 20% dimethylsulfoxide. The rats were divided into four groups and zonisamide was administered 24 h after 6-hydroxydopamine (as mentioned briefly in Supplementary material, Table 3C). One week after 6-hydroxydopamine administration, the brains assigned for qRT-PCR were harvested, and the mesencephalon containing the substantia nigra (midbrain delineated longitudinally 4.6–6.6 mm from the bregma, perpendicularly less than 7 mm from the skull; Paxinos and Watson, 2009) was dissected out and stored at −80 °C until assayed by qRT-PCR.

2.6. qRT-PCR

Primary cortical astrocytes and samples of ventral mesencephalic containing substantia nigra were processed for qRT-PCR as described previously (Choudhury et al., 2011b). Briefly, the cells were lysed using ISOGEN (Nippon Gene, Co. Ltd., Tokyo, Japan) followed by 10 times passage of the lysate through a micropipette and, in the case of brain tissue, the samples were homogenized into lysate using an ultrasonic cell culture disruptor. Then, their total RNA was collected using the trizol protocol and cDNA was obtained from DNase-I-treated RNA by reverse transcription using an oligo-(dT) 15 primer. qRT-PCR analysis was performed in triplicate using an MJ mini instrument (BioRad, Hercules, CA, USA) using Fast StartUniversal SYBR Green (Roche Diagnostic Japan). PCR conditions were as follows: 50 °C for 2 min, 95 °C for 10 min, followed by 40 cycles at 95 °C for 15 s, and 60 °C for

1 min. All gene-specific mRNA expression values were normalized against β-actin mRNA. The primer sequences for each gene, as well as the sizes of their products, source, are described in Supplementary material, Table 2.

2.7. Immunoblotting

The brain slices for immunoblotting study were prepared as described previously (Tanaka et al., 1998) with slight changes in gel transfer as here we used a Trans-Blot Turbo transfer system (Bio-Rad Laboratories, CA, USA). Briefly, the organotypic culture was washed with PBS and homogenized with SDS solution in 10 volumes of Laemmli's sample solution containing 3% SDS. The lysates were electrophoresed, transferred to nitrocellulose membranes and immunoblotted with antibodies to β-actin and tyrosine hydroxylase (Supplementary material, Table 3). The immunoreaction was visualized using nitro blue tetrazolium and 5-bromo-4-chloro-3-indolyl phosphate and immunoreactive bands were analyzed by densitometry using ImageJ 1.43u (Wayne Rasband, National Institute of Health, Bethesda, ML, USA). The densitometry data were standardized using β-actin as an internal standard.

2.8. Immunofluorescence

The primary antibodies listed in Supplementary material, Table 2 were used for indirect immunofluorescence staining (Yokoyama et al., 2006). Briefly, anesthetized rats were fixed by transcardial perfusion with 4% paraformaldehyde containing 2 mM $MgCl_2$ for 10 min, at a flow rate of 80 ml/min. The dissected brains were immersed in 15% sucrose in PBS at 4 °C overnight, rapidly frozen in dry ice powder, and sliced into 10 μm-thick coronal sections at the level of the substantia nigra level (4.80–5.40 mm from the bregma). The brain sections were incubated with the primary antibodies to tyrosine hydroxylase, S100β, and glial fibrillary acidic protein (Supplementary material, Table 3) followed by incubation with DyLight 488, DyLight 549, and/or DyLight 649-labeled secondary antibodies (Jackson ImmunoResearch Laboratories, West Grove, PA, USA). Hoechst 33258 (Sigma Chemical Co.) was used for nuclear staining. The immunostained specimens were observed with a Nikon A1 confocal laser scan microscope (Tokyo, Japan) using a 20× objective lens. The area observed was 2.0–2.3 mm lateral from the midline. Cells numbers were counted manually under blind conditions, i.e., with the observer being unaware of group allocation of the sections.

2.9. Statistical analysis

For statistical analysis, one-way analysis of variance was used and multiple comparisons were corrected for using the Tukey test. Results with P values <0.05 were considered statistically significant. All results are expressed as mean values ± standard error of the mean (S.E.M.).

3. Results

3.1. Zonisamide increased the expression of anti-oxidative factors

To look for direct evidence whether the increased number of astrocytes induced by zonisamide administration (Asanuma et al., 2010; Choudhury et al., 2011a) might protect against the 6-hydroxydopamine-induced oxidative stress of dopamine neurons, we performed qRT-PCR with the primers of various anti-oxidative factors. We found that zonisamide (1, 10, and 100 μM) treatment of primary astrocyte cultures significantly increased metallothionein-2 mRNA ($P<0.001$ vs. control; Fig. 1A). Zonisamide post-treatment following 6-hydroxydopamine treatment also significantly up-regulated metallothionein-2 mRNA content ($P<0.01$ vs. 6-hydroxydopamine+saline; Fig. 2A). In compare to saline group, zonisamide alone increased the metallothionein-2 mRNA content ($P<0.001$ vs. saline; Fig. 2A).

Moreover, zonisamide (10 and 100 μM) significantly increased the expression of copper/zinc superoxide dismutase (Cu/ZnSOD) in primary astrocyte cultures ($P<0.001$ vs. control; Fig. 1B) and the significant up-regulation of Cu/ZnSOD mRNA in 6-hydroxydopamine-treated substantia nigra were also observed in our *in vivo* study, where the animals were treated with zonisamide (30 mg/kg) for 7 consecutive days ($P<0.001$ vs. 6-hydroxydopamine+saline; Fig. 2B).

Consistent with a previous report (Kawajiri et al., 2010), we also found that zonisamide post-treatment after 6-hydroxydopamine treatment increased the expression of manganese superoxide dismutase (MnSOD) mRNA in 6-hydroxydopamine-treated substantia nigra ($P<0.05$ vs. 6-hydroxydopamine+saline; Fig. 2C). In the primary astrocyte cell culture study, we found that the exposure of primary astrocytes cultures to zonisamide (10 and 100 μM) also caused up-regulation of MnSOD mRNA ($P<0.05$ vs. control; Fig. 1C).

3.2. Zonisamide increased the expression of neurotrophic factors

Given the apparent astrocyte-mediated neurotrophic effects of zonisamide (Asanuma et al., 2010; Choudhury et al., 2011a), we next investigated whether astrocyte-derived neurotrophic/growth factors are increased by administration of zonisamide and might therefore mediate a neuroprotective function. To that end, we quantified the expression of mRNA encoding various neurotrophic factors.

Interestingly, qRT-PCR analysis revealed that the treatment of cortical astrocytes with zonisamide (1, 10, and 100 μM) increased mesencephalic astrocyte-derived neurotrophic factor mRNA levels ($P<0.01$ vs. control; Fig. 1D) and zonisamide post-treatment following 6-hydroxydopamine treatment increased the content of mRNA encoding mesencephalic astrocyte-derived neurotrophic factor in substantia nigra ($P<0.01$ vs. 6-hydroxydopamine+saline; Fig. 2D). Indeed, 6-hydroxydopamine treatment increased the contents of mesencephalic astrocyte-derived neurotrophic factor mRNA ($P<0.05$ vs. saline; Fig. 2D) but the 6-hydroxydopamine-induced up-regulation of mesencephalic astrocyte-derived neurotrophic factor mRNA was accelerated by zonisamide post-treatment.

Although the expression of mRNA encoding vascular endothelial growth factor of zonisamide-treated astrocytes cultures was not up-regulated even at the high concentration of 100 μM zonisamide (Fig. 1E), a massive increase in the content of vascular endothelial growth factor mRNA was found in substantia nigra following post-treatment with zonisamide 24 h after 6-hydroxydopamine exposure ($P<0.001$ vs.6-hydroxydopamine+saline; Fig. 2E).

3.3. Zonisamide increased the expression of proliferative factors

It has been reported that proliferating cell nuclear antigen is a hallmark of the reactive astrocytic proliferation (Miyake et al., 1992) and a previous study has shown that zonisamide increases the number of astrocytes (Choudhury et al., 2011a). To further examine this, we performed qRT-PCR using the primer for proliferating cell nuclear antigen. This demonstrated that the treatment of primary astrocyte cultures with zonisamide (1, 10, and 100 μM) significantly ($P<0.001$ vs. control; Fig. 1F) upregulated the expression of mRNA encoding proliferating cell nuclear antigen. Beside this, in our *in vivo* study, *zonisamide* post-treatment also significantly

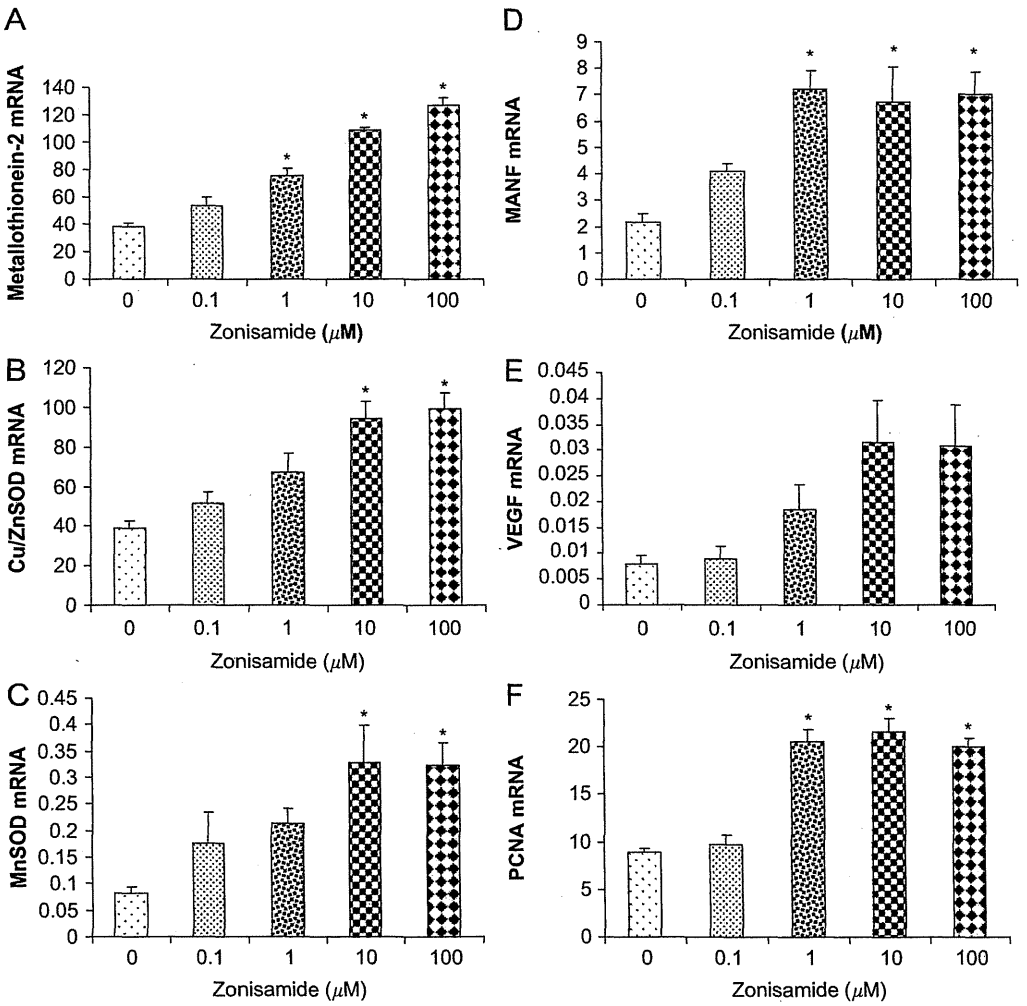

Fig. 1. Effects of zonisamide (ZNS) on cultured astrocytes and its concentration dependency. qRT-PCR revealed that primary cultured astroglial mRNAs encoding anti-oxidative factors [(A) metallothionein-2, (B) copper/zinc superoxide dismutase (Cu/ZnSOD), and (C) manganese superoxide dismutase (MnSOD)] and neurotrophic factors [(D) mesencephalic astrocyte-derived neurotrophic factor (MANF), (E) vascular endothelial growth factor (VEGF), and (F) proliferating cell nuclear antigen (PCNA)] were increased with exposure to zonisamide. The level of significance was analyzed by ANOVA with *post-hoc* Tukey test. Data are expressed as mean ± S.E.M. ($n=4$ per group). $^{*}P<0.05$; $^{**}P<0.01$; and $^{***}P<0.001$ vs. control (zonisamide untreated).

increased the mRNA content of proliferating cell nuclear antigen in 6-hydroxydopamine-treated substantia nigra ($P<0.001$ vs. 6-hydroxydopamine+saline; Fig. 2F). In compare to saline group, zonisamide only increased the mRNA encoding proliferating cell nuclear antigen ($P<0.01$ vs. saline; Fig. 2F).

3.4. Zonisamide post-treatment attenuated 6-hydroxydopamine-induced dopaminergic neuronal loss

For evaluation of the morphological features of dopamine neurons following the different 6-hydroxydopamine treatments, detailed microscopic analyses were conducted using the confocal laser scan microscopy images of tyrosine hydroxylase immunofluorescence. Treatment with 6-hydroxydopamine produced a remarkable reduction of tyrosine hydroxylase-positive neurons to 25% of the normal control group ($P<0.001$ vs. saline; Fig. 3A). Zonisamide post-treatment increased the number of tyrosine hydroxylase-positive neurons by 172% as compared to the group receiving 6-hydroxydopamine alone ($P<0.001$ vs. 6-hydroxydopamine+saline; Fig. 3A).

3.5. Zonisamide increased the number of S100β-positive cells

S100β is primarily secreted by a subtype of mature astrocytes and extracellular S100β exerts autocrine effects that promote astrocyte proliferation (Selinfreund et al., 1991; Donato, 2003). The number of S100β positive cells in the area of substantia nigra was increased by 6-hydroxydopamine treatment by 106% of normal controls (Fig. 4B). Similar to our previous MPTP study, here we also found that zonisamide post-treatment after 6-OHDA increased the number of S100β-positive cells by 27% of 6-hydroxydopamine-treated group and zonisamide-treatment only increased the number of S100β-positive cells by 55% normal control group (Fig. 3B).

3.6. Zonisamide did not increase the number of GFAP-positive astrocytes

In regards, GRAP-positive astrocytes, the scenario of 6-hydroxydopamine-treament was similar to that of S100β where by the number of GFAP-positive astrocyte was increased by 339% of normal control (Fig. 3C). But zonisamide treatment did not show

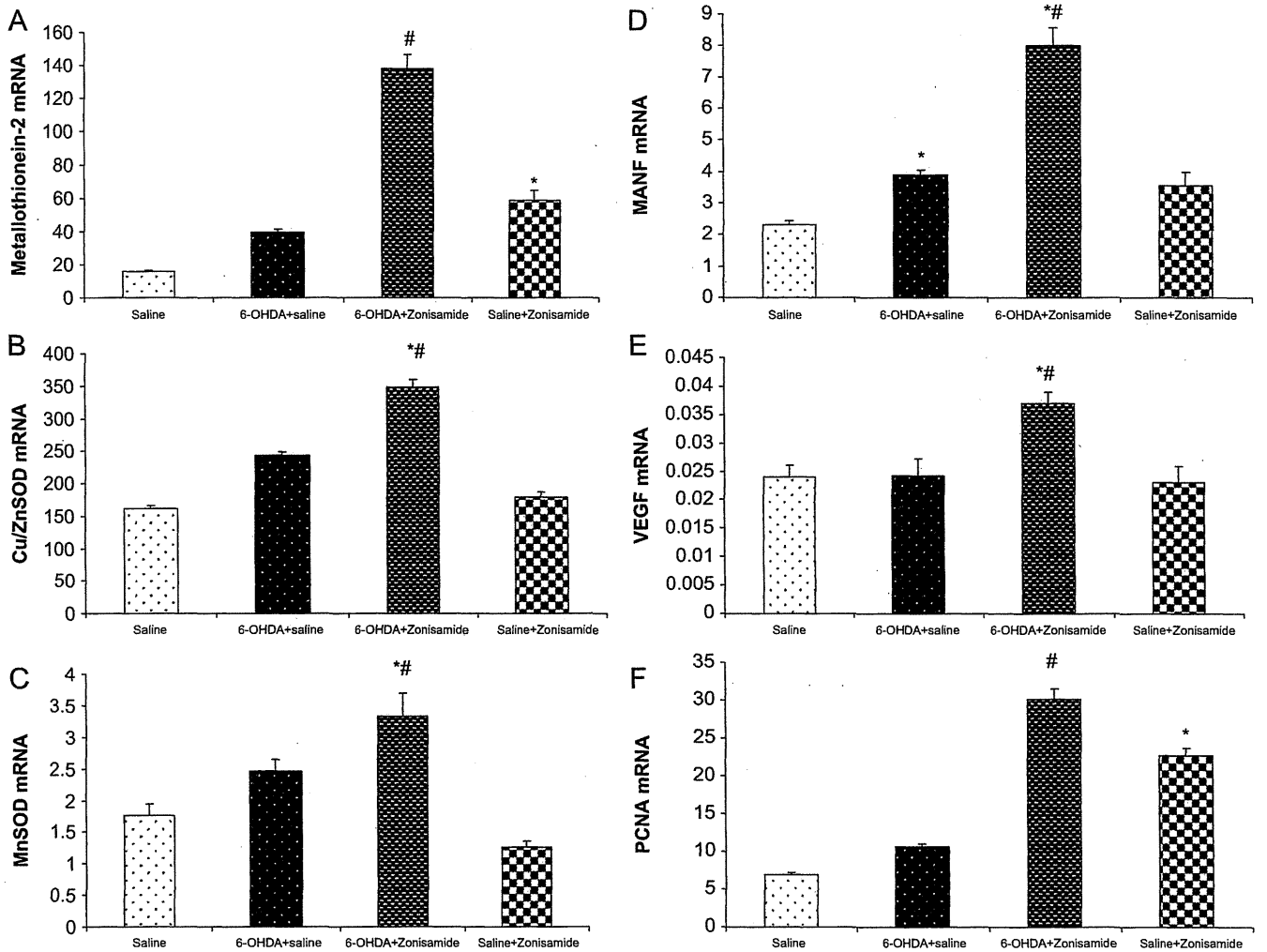

Fig. 2. Effects of repeated administration of zonisamide (ZNS) on mRNA expressions in substantia nigra of rats treated with saline (normal control), 6-hydroxydopamine (6-OHDA)+saline [6-OHDA 50 μg/rat followed by saline 100 μl/rat × 7 every 24 h]; 6-OHDA+ZNS [6-OHDA followed by ZNS 30 mg/kg × 7 every 24 h]; and saline+ZNS [saline 5 μl/rat followed by ZNS × 7 every 24 h]; the mRNA content of anti-oxidative factors [(A) metallothionein-2, (B) copper/zinc superoxide dismutase (Cu/ZnSOD), and (C) manganese superoxide dismutase (MnSOD)] and neurotrophic factors [(D) mesencephalic astrocyte-derived neurotrophic factor (MANF), (E) vascular endothelial growth factor (VEGF), and (F) proliferating cell nuclear antigen (PCNA)] were increased in 6-hydroxydopamine-treated substantia nigra with post-administration of zonisamide at the dose of 30 mg/kg once daily for 7 day. The level of significance were analyzed by ANOVA with *post-hoc* Tukey test. Data are expressed as mean ± S.E.M. (n=4 per group). $^{*}P < 0.05$ vs. saline; $^{\#}P < 0.05$ vs. 6-hydroxydopamine+saline.

any effects (Fig. 3C) on 6-hydroxydopamine-induced increased number of GFAP-positive astrocyte.

3.7. Zonisamide pre-treatment attenuated the depletion of mesencephalic tyrosine hydroxylase contents by 6-hydroxydopamine-induced toxicity

To assess the neuroprotective properties of zonisamide, we treated organotypic slice cultures of substantia nigra from rat midbrains with various concentrations of zonisamide (0, 0.1, 1, 10, and 100 μM) 24 h prior to exposure with 6-hydroxydopamine plus N-methyl-D-aspartic acid. The viability of dopaminergic neurons was assessed by tyrosine hydroxylase immunoblotting. Zonisamide suppressed the degeneration of dopaminergic neurons in 6-hydroxydopamine-treated midbrain slices, as revealed by immunoblotting with an antibody to tyrosine hydroxylase (Fig. 4). Following incubation with various concentrations of zonisamide (0, 0.1, 1, 10, and 100 μM) for 24 h, slices were exposed to a mixture of 6-hydroxydopamine and N-methyl-D-aspartic acid for 48 h. Exposure to the neurotoxic mixture reduced tyrosine hydroxylase protein content in the slices. Pre-treatment with a high concentration of zonisamide (100 μM) significantly attenuated 6-hydroxydopamine-induced depletion of tyrosine hydroxylase content, ($P < 0.01$ vs. 6-hydroxydopamine+saline), while low concentrations of zonisamide (0.1 and 1 μM) did not elicit significant neuroprotective effects (Fig. 4).

4. Discussion

Dopaminergic neuronal loss is primarily responsible for the onset and progression of Parkinson's disease. Thus, neuroprotective and/or neuroregenerative strategies remain critical to the treatment of this increasingly prevalent disease. Zonisamide has been introduced by a clinical trial as an effective treatment for Parkinson's disease (Murata et al., 2007). Recently, it has been reported that zonisamide offers astrocyte-mediated neuroprotection against 6-hydroxydopamine-induced neurotoxicity by suppressing oxidative stress (Asanuma et al., 2010). The astrocyte-mediated neuroprotection of zonisamide was also confirmed

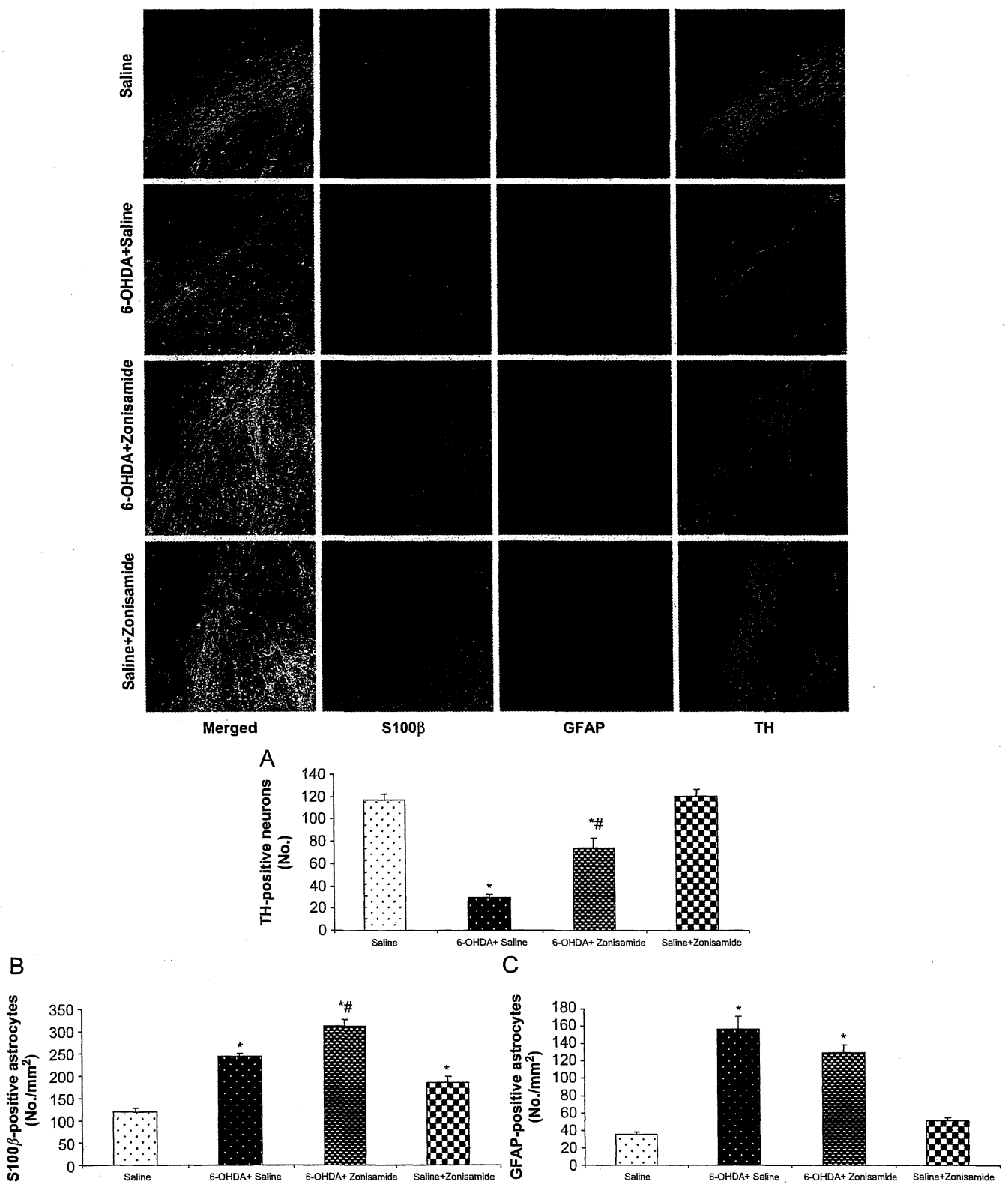

Fig. 3. Images show triple-immunostained substantia nigra of rats (at 1 week) belonging to the saline, 6-hydroxydopamine (6-OHDA)+saline, 6-OHDA+zonisamide (ZNS) and saline+ZNS groups (as described in Fig. 3) with antibodies to tyrosine hydroxylase (TH) [red], S100β (green), glial fibrillary acidic protein (GFAP) [pink], and merged images. Bar scale, 100 μm. The number of (A) TH-positive neurons, (B) S100 β-positive astrocytes, and (C) GFAP-positive astrocytes in the substantia nigra of different treated groups. The level of significance were analyzed by ANOVA with *post-hoc* Tukey test. Data are expressed as mean ± S.E.M. ($n=4$ per group). *$P<0.05$ vs. saline; #$P<0.05$ vs. 6-hydroxydopamine+saline.

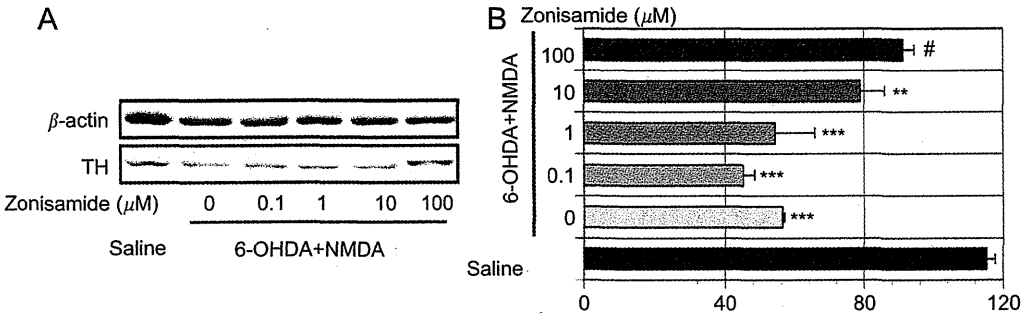

Fig. 4. Neuroprotective effects of zonisamide (ZNS) on 6-hydroxydopamine (6-OHDA)-induced tyrosine hydroxylase (TH) protein depletion where N-methyl-D-aspartic acid were used for excitotoxic stimulation. The protective effects of zonisamide were revealed by tyrosine hydroxylase immunoblotting in mesencephalic slices treated with 6-hydroxydopamine and N-methyl-D-aspartic acid. (A) Representative immunoblot data ($n=1$) showing tyrosine hydroxylase and β-actin protein levels at 48 h after exposure to 6-hydroxydopamine and N-methyl-D-aspartic acid (100 μM). (B) Densitometric analysis of the immunoblot data are presented as the mean ± S.E.M. ($n=3$ per group). The level of significance were analyzed by ANOVA with *post-hoc* Tukey test. $^{*}P<0.05$; $^{**}P<0.01$; and $^{***}P<0.001$ vs. saline; $^{\#}P<0.05$ vs. 6-hydroxydopamine+N-methyl-D-aspartic acid.

against MPTP-treated mice (Choudhury et al., 2011a). Astrocytes have strong antioxidant properties (Tanaka et al., 1999) and protect dopamine neurons from the 6-hydroxydopamine-induced oxidative stress by releasing metallothioneins (Miyazaki et al., 2011). On oxidative stress, astrocytes express NF-E2-related factor (Nrf2), which binds to the antioxidant response element to release antioxidant enzymes (Jakel et al., 2007), suggesting an important approach by which cells defend themselves against oxidative stress. The current study provides further evidence that the protective effects of zonisamide towards dopamine neurons in the substantia nigra are mediated through its actions on astrocytes by enhancing their expression of mRNA encoding neurotrophic factors and anti-oxidative factors.

Metallothioneins are a family of cysteine-rich proteins, an experimental data suggest that they may provide protection against oxidative stress (Kumari et al., 1998). In our study, 6-hydroxydopamine-treament activated the astrocytes residing around the area of damaging substantia nigra of the mid-brain where astroglial activation may be induced by the oxidative stress of dopaminergic neurons and the activated astrocytes seems to up-regulate mRNA encoding metallothionein-2 (Fig. 2A). Similar impression was found in a recent report (Miyazaki et al., 2011), where the up-regulation of metallothionein may be due to self defending mechanism of neurons and astrocytes against oxidative stress. Our findings suggested, the up-regulation of mRNA encoding metallothionein-2 resulted by the cross talk between the damaged dopamine neurons and astrocytes in response to 6-hydroxydopamine, the up-regulations mRNA encoding metallothionein-2 by 6-hydroxydopamine was accelerated by zonisamide post-treatment (Fig. 2A) and a recent study also supported our evidence where zonisamide protected dopamine neurons by suppressing caspase-3 activity (Omura et al., 2011) as the metallothioneins prevent neuronal death (Hashimoto et al., 2011) by reducing the activity of caspase-3 and content of tumor necrosis factor-α (Helal et al., 2009). Thus, zonisamide may act in our current study on astrocytes to produce metallothioneins, which may in turn promote dopaminergic neuronal survival by suppressing 6-hydroxydopamine-induced oxidative stress and the activity of caspase-3. Moreover, astrocytes enhance defenses against free radicals in capillary endothelial cells by up-regulation of other anti-oxidative factors namely MnSOD and Cu/ZnSOD (Schroeter et al., 1999), which are also activated in response to neuronal damage, and these activated astrocytes may help neurons to recover from neuronal damage (Kato et al., 1994; Ridet et al., 1997). In our study, the scenarios of MnSOD and Cu/ZnSOD in response to 6-hydroxydopamine-treament presented similar impression as we observed in metallothionein-2 where 6-OHDA-treated astrocytes in substantia nigra most likely also increased the contents of mRNA encoding MnSOD and Cu/ZnSOD for self defense mechanism of neuro-astroglial crosstalk (Figs. 2B and C). MnSOD is an anti-oxidant localized in mitochondria, which represents a defense against the oxidative stress mediated by the free radicals released in the mitochondria and over-expression of MnSOD attenuates MPTP-toxicity and also protects cellular apoptosis (Manna et al., 1998; Zhao et al., 2001). Moreover, MnSOD-overexpressing transgenic mice are more resistant to MPTP-toxicity (Klivenyi et al., 1998). Zonisamide has been shown to increase the viability of SH-SY5Y cells through up-regulation of MnSOD (Kawajiri et al., 2010).

Astrocytes, additionally, have been shown to secrete a number of neurotrophic factors for injured dopaminergic neurons (Saavedra et al., 2006; Chen et al., 2006; Petrova et al., 2003). Mesencephalic astrocyte-derived neurotrophic factor is responsible for intracellular protection against the Bax-dependent apoptosis (Hellman et al., 2011) and suppresses 6-hydroxydopamine toxicity against dopaminergic neurons (Voutilainen et al., 2009). Of particular interest, in response to endoplasmic reticulum stress due to 6-hydoxydopamine, increased production of mesencephalic astrocyte-derived neurotrophic factor (Tadimalla et al., 2008) also suggesting an important self repairing mechanism of injured brain tissues where the increased amount of glial cells-derived other neurotrophic factors may help on injured neurons to recover (Asanuma et al., 2010; Choudhury et al., 2011a,b; Kitamura et al., 2010). In this study, we presented same evidence where up-regulation of mesencephalic astrocyte-derived neurotrophic factor's mRNA was found in response to 6-hydoxydopamine (Fig. 2D). Zonisamide may aid the activated astrocytes to stimulate the repairing mechanism of nigral tissues. Moreover, an interesting study represented the astrocytic activating effects of zonisamide having an interpretation about the possibility of increase neurotrophic effects (Asanuma et al., 2010). Likely, we also added the evidence by showing the up-regulation of mesencephalic astrocyte-derived neurotrophic factor induced by zonisamide. In addition to mesencephalic astrocyte-derived neurotrophic factor, the ubiquitous growth factor namely vascular endothelial growth factor shown to be neuroprotective towards neuronal degeneration (Poesen et al., 2008; Falk et al., 2009). Notably, vascular endothelial growth factor has been demonstrated to inhibit apoptosis and has only minimal angiogenic activity (Li et al., 2008). It also acts as a critical factor for promoting survival of dopaminergic neurons in the 6-hydroxydopamine-treated midbrain (Yasuhara et al., 2004; Yasuhara et al., 2005). In line with this, our study addressed another impression about activated astrocyte-derived neurotrophic factors where neither zonisamide nor 6-hydroxydopamine

did up-regulate vascular endothelial growth factor (Figs. 1E and 2E) whereas, zonisamide post-treatment after 6-hydroxydopamine increased the levels of mRNA encoding vascular endothelial growth factor (Fig. 2E). Here, we interpret that the stimulation by neurotoxin for the synthesis of vascular endothelial growth factor may require higher degree than that of mesencephalic astrocyte-derived neurotrophic factor as the up-regulation of vascular endothelial growth factor were observed brain injury (Koyama and Michinaga, 2012). Unlikely mesencephalic astrocyte-derived neurotrophic factor, the stimulation of zonisamide on resting astrocytes (6-hydroxydopamine-nontreated) may not able to increase the significant amount mRNA encoding vascular endothelial growth factor. Although, the synergistic effects of 6-hydroxydopamine and zonisamide may produce sufficient amount of mRNA encoding vascular endothelial growth factor where 6-hydroxydopamine induced stress may activate the astrocyte and zonisamide may acts on activated astrocyte for producing significant amount of vascular endothelial growth factor.

Zonisamide has recently been reported to increase the number of S100β positive astrocytes but not GFAP positive astrocytes in C6 cell culture (Asanuma et al., 2010) and in the substantia nigra of MPTP-treated mice (Choudhury et al., 2011a), the evidences suggest that GFAP-positive astrocyte works to remove dead cells with their jeopardizing effects by releasing reactive oxygen species, cytokines, chemokines, prostaglandins (Yokoyama et al., 2011). By contrast, S100β-positive astrocytes played neurotrophic effects for repairing damaged cells as S100β is selectively expressed in astrocytes, having autocrine effects that promote astrocyte proliferation (Donato, 2003; Selinfreund et al., 1991). S100β also has neurotrophic actions, including neurite outgrowth, neuron survival, and protection against glucose deprivation and excitotoxicity (Van Eldik and Wainwright, 2003). It might also be involved in the cellular defense mechanism against oxidative stress (Migheli et al., 1999). Indeed, both GRAP positive astrocytes and S100β-positive astrocytes are shown to increase in response to neurotoxin with different characteristics (Himeda et al., 2006). In agreement with these studies, our Parkinson's disease model also showed that 6-hydroxydopamine increased the number of S100β positive astrocytes not GFAP-positive astrocytes for repairing the injured dopamine neurons and zonisamide may promote the cellular defense mechanism by proliferation of S100β positive astrocytes for protecting injured dopamine neurons (Himeda et al., 2006). Notably, zonisamide markedly up-regulated the mRNA of indicating maker for proliferation namely proliferating cell nuclear antigen *in vitro* and *in vivo* (Figs. 1F and 2F) as it has been reported that an increased level of proliferating cell nuclear antigen is a hallmark of reactive astrocytic proliferation (Miyake et al., 1992). Zonisamide may acts on the activated astrocytes to accelerate the defending mechanism of nigral cells and also may have the ability to activate S100β positive astrocytes (Asanuma et al., 2010; Choudhury et al., 2011a).

In deed, we confirmed the neuroprotective effect of zonisamide prior to 6-hydroxydopamine lesion in our slice culture study. But we employed zonisamide post-treatment after 6-hydroxydopamine with priority, to study the events (neurotrophic and anti-oxidative effects) of the crosstalk between injured dopamine neurons and activated astrocytes in the condition of Parkinson's disease patients. As we aimed to suggest the clinical neurologist for prescribing zonisamide to our Parkinson's disease patient to slow down the process of neurodegeneration where by the dopamine neurons are already injured or damaged. In one hand, our current study suggesting that zonisamide strengthened the neuroprotective functions of astrocytes, including the production of anti-oxidative and neurotrophic factors. On the other hand, zonisamide did not elicit significant effects on microglial cells (data not shown), which also have neuroprotective effects that are mediated at least in part by releasing neurotrophic substances (Kitamura et al., 2010; Choudhury et al., 2011b). These findings suggesting the identification of therapeutic agents that may induce the phenotypic alterations of glial cells surrounding degenerating dopaminergic neurons in the substantia nigra is a promising strategy for neuroprotective therapies for Parkinson's disease.

5. Conclusion

The major findings of our current studies are the identification of zonisamide-mediated astrocyte-derived anti-oxidative and neurotrophic factor's mRNAs. These effects of zonisamide may potentiate the astrocyte derived adaptive immune arm for dopamine neuronal survival in our Parkinson's disease models. These data may suggest anti-oxidative and neurorotrophic effects of zonisamide, although respective protein assay may be needed to establish this conclusion. These emerging roles of zonisamide towards astrocytes in the pathogenesis of Parkinson's disease may constitute an exciting development with a promise for novel therapeutics.

Acknowledgments

The authors wish to acknowledge the Grant-in-Aid from the Research Committee of Parkinson's disease, the Ministry of Health, Labor and Welfare of Japan and GJTS for their financial support for conducting our study. Mohammed Emamussalehin Choudhury is supported by Japanese Government Scholarship (Monbukagakusho: Ministry of Education, Culture, Sports, Science, and Technology, Japan).

Appendix A. Supplementary material

Supplementary data associated with this article can be found in the online version at http://dx.doi.org/10.1016/j.ejphar.2012.05.012.

References

Asanuma, M., Miyazaki, I., Diaz-Corrales, F.J., Kimoto, N., Kikkawa, Y., Takeshima, M., Miyoshi, K., Murata, M., 2010. Neuroprotective effects of zonisamide target astrocyte. Ann. Neurol. 67, 239–249.

Asanuma, M., Miyazaki, I., Diaz-Corrales, F.J., Miyoshi, K., Ogawa, N., Murata, M., 2008. Preventing effects of a novel anti-parkinsonian agent zonisamide on dopamine quinone formation. Neurosci. Res. 60, 106–113.

Bermejo, P.E., Ruiz-Huete, C., Anciones, B., 2010. Zonisamide in managing impulse control disorders in Parkinson's disease. J. Neurol. 257, 1682–1685.

Chen, P.S., Peng, G.S., Li, G., Yang, S., Wu, X., Wang, C.C., Wilson, B., Lu, R.B., Gean, P.W., Chuang, D.M., Hong, J.S., 2006. Valproate protects dopaminergic neurons in midbrain neuron/glia cultures by stimulating the release of neurotrophic factors from astrocytes. Mol. Psychiatry 11, 1116–1125.

Choudhury, M.E., Moritoyo, T., Kubo, M., Kyaw, W.T., Yabe, H., Nishikawa, N., Nagai, M., Matsuda, S., Nomoto, M., 2011a. Zonisamide-induced long-lasting recovery of dopaminergic neurons from MPTP-toxicity. Brain Res. 1384, 170–178.

Choudhury, M.E., Moritoyo, T., Yabe, H., Nishikawa, N., Nagai, M., Kubo, M., Matsuda, S., Nomoto, M., 2010. Zonisamide attenuates MPTP neurotoxicity in marmosets. J. Pharmacol. Sci. 114, 298–303.

Choudhury, M.E., Sugimoto, K., Kubo, M., Nagai, M., Nomoto, M., Takahashi, H., Yano, H., Tanaka, J., 2011b. A cytokine mixture of GM-CSF and IL-3 that induces a neuroprotective phenotype of microglia leading to amelioration of 6-OHDA-induced Parkinsonism of rats. Brain Behav. 1, 26–43.

Costa, C., Tozzi, A., Luchetti, E., Siliquini, S., Belcastro, V., Tantucci, M., Picconi, B., Ientile, R., Calabresi, P., Pisani, F., 2010. Electrophysiological actions of zonisamide on striatal neurons: selective neuroprotection against complex I mitochondrial dysfunction. Exp. Neurol. 221, 217–224.

Donato, R., 2003. Intracellular and extracellular roles of S100 proteins. Microsc. Res. Tech. 60, 540–551.

Falk, T., Zhang, S., Sherman, S.J., 2009. Vascular endothelial growth factor B (VEGF-B) is up-regulated and exogenous VEGF-B is neuroprotective in a culture model of Parkinson's disease. Mol. Neurodegener. 4, 49.

Hashimoto, K., Hayashi, Y., Watabe, K., Inuzuka, T., Hozumi, I., 2011. Metallothionein-III prevents neuronal death and prolongs life span in amyotrophic lateral sclerosis model mice. Neuroscience 189, 293–298.
Helal, G.K., Aleisa, A.M., Helal, O.K., Al-Rejaie, S.S., Al-Yahya, A.A, Al-Majed, A.A., Al-Shabanah, O.A., 2009. Metallothionein induction reduces caspase-3 activity and TNFalpha levels with preservation of cognitive function and intact hippocampal neurons in carmustine-treated rats. Oxid. Med. Cell. Longev. 2, 26–35.
Hellman, M., Arumäe, U., Yu, L.Y., Lindholm, P., Peränen, J., Saarma, M., Permi, P., 2011. Mesencephalic astrocyte-derived neurotrophic factor (MANF) has a unique mechanism to rescue apoptotic neurons. J. Biol. Chem. 286, 2675–2680.
Himeda, T., Watanabe, Y., Tounai, H., Hayakawa, N., Kato, H., Araki, T., 2006. Time dependent alterations of co-localization of S100beta and GFAP in the MPTP-treated mice. J. Neural Transm. 113, 1887–1894.
Iijima, M., Osawa, M., Kobayashi, M., Uchiyama, S., 2011. Efficacy of zonisamide in a case of Parkinson's disease with intractable resting and re-emergent tremor. Eur. J. Neurol. 18, 43–44.
Jakel, R.J., Townsend, J.A., Kraft, A.D., Johnson, J.A., 2007. Nrf2-mediated protection against 6-hydroxydopamine. Brain Res. 1144, 197–201.
Kato, H., Kogure, K., Araki, T., Itoyama, Y., 1994. Astroglial and microglial reactions in the gerbil hippocampus with induced ischemic tolerance. Brain Res. 664, 69–76.
Kawajiri, S., Machida, Y., Saiki, S., Sato, S., Hattori, N., 2010. Zonisamide reduces cell death in SH-SY5Y cells via an anti-apoptotic effect and by upregulating MnSOD. Neurosci. Lett. 481, 88–91.
Kitamura, Y., Inden, M., Minamino, H., Abe, M., Takata, K., Taniguchi, T., 2010. The 6-hydroxydopamine-induced nigrostriatal neurodegeneration produces microglia-like NG2 glial cells in the rat substantia nigra. Glia 58, 1686–1700.
Klivenyi St, P., Clair, D., Wermer, M., Yen, H.C., Oberley, T., Yang, L., Flint Beal, M., 1998. Manganese superoxide dismutase overexpression attenuates MPTP toxicity. Neurobiol. Dis. 5, 253–258.
Koyama., Y., Michinaga, S., 2012. Regulations of astrocytic functions by endothelins: roles in the pathophysiological responses of damaged brains. J. Pharmacol. Sci. 118, 401–407.
Kress, G.J., Reynolds, I.J., 2005. Dopaminergic neurotoxins require excitotoxic stimulation in organotypic cultures. Neurobiol. Dis. 20, 639–645.
Kumari, M.V., Hiramatsu, M., Ebadi, M., 1998. Free radical scavenging actions of metallothionein isoforms I and II. Free Radical Res. 29, 93–101.
Li, Y., Zhang, F., Nagai, N., Tang, Z., Zhang, S., Scotney, P., Lennartsson, J., Zhu, C., Qu, Y., Fang, C., Hua, J., Matsuo, O., Fong, G.H., Ding, H., Cao, Y., Becker, K.G., Nash, A., Heldin, C.H., Li, X., 2008. VEGF-B inhibits apoptosis via VEGFR-1-mediated suppression of the expression of BH3-only protein genes in mice and rats. J. Clin. Invest. 118, 913–923.
Manna, S.K., Zhang, H.J., Yan, T., Oberley, L.W., Aggarwal, B.B., 1998. Overexpression of manganese superoxide dismutase suppresses tumor necrosis factor-induced apoptosis and activation of nuclear transcription factor-kappaB and activated protein-1. J. Biol. Chem. 273, 13245–13254.
Migheli, A., Cordera, S., Bendotti, C., Atzori, C., Piva, R., Schiffer, D., 1999. S-100beta protein is upregulated in astrocytes and motor neurons in the spinal cord of patients with amyotrophic lateral sclerosis. Neurosci. Lett. 261, 25–28.
Miyake, T., Okada, M., Kitamura, T., 1992. Reactive proliferation of astrocytes studied by immunohistochemistry for proliferating cell nuclear antigen. Brain Res. 590, 300–302.
Miyazaki, I., Asanuma, M., Kikkawa, Y., Takeshima, M., Murakami, S., Miyoshi, K., Sogawa, N., Kita, T., 2011. Astrocyte-derived metallothionein protects dopaminergic neurons from dopamine quinone toxicity. Glia 59, 435–451.
Murata, M., Hasegawa, K., Kanazawa, I., Japan Zonisamide on PD Study Group, 2007. Zonisamide improves motor function in Parkinson disease: a randomized, double-blind study. Neurology 68, 45–50.
Omura, T., Asari, M., Yamamoto, J., Kamiyama, N., Oka, K., Hoshina, C., Maseda, C., Awaya, T., Tasaki, Y., Shiono, H., Shimizu, K., Matsubara, K., 2011. HRD1 levels increased by zonisamide prevented cell death and caspase-3 activation caused by endoplasmic reticulum stress in SH-SY5Y cells. J. Mol. Neurosci. 46, 527–535.
Paxinos, G., Watson, C., 2009. The rat brain in stereotaxic coordinates: compact, sixth edition Academic Press.
Petrova, P., Raibekas, A., Pevsner, J., Vigo, N., Anafi, M., Moore, M.K., Peaire, A.E., Shridhar, V., Smith, D.I., Kelly, J., Durocher, Y., Commissiong, J.W., 2003. MANF: a new mesencephalic, astrocyte-derived neurotrophic factor with selectivity for dopaminergic neurons. J. Mol. Neurosci. 20, 173–188.
Poesen, K., Lambrechts, D., Van Damme, P., Dhondt, J., Bender, F., Frank, N., Bogaert, E., Claes, B., Heylen, L., Verheyen, A., Raes, K., Tjwa, M., Eriksson, U., Shibuya, M., Nuydens, R., Bosch, L., Meert, T., D'Hooge, R., Sendtner, M., Robberecht, W., Carmeliet, P., 2008. Novel role for vascular endothelial growth factor (VEGF) receptor-1 and its ligand VEGF-B in motor neuron degeneration. J. Neurosci. 28, 10451–10459.
Ridet, J.L., Malhotra, S.K., Privat, A., Gage, F.H., 1997. Reactive astrocytes: cellular and molecular cues to biological function. Trends Neurosci. 20, 570–577.
Saavedra, A., Baltazar, G., Santos, P., Carvalho, C.M., Duarte, E.P., 2006. Selective injury to dopaminergic neurons up-regulates GDNF in substantía nigra postnatal cell cultures: role of neuron-glia crosstalk. Neurobiol. Dis. 23, 533–542.
Schroeter, M.L., Mertsch, K., Giese, H, Müller, S., Sporbert, A., Hickel, B., Blasig, I.E., 1999. Astrocytes enhance radical defence in capillary endothelial cells constituting the blood–brain barrier. FEBS Lett. 449, 241–244.
Selinfreund, R.H., Barger, S.W., Pledger, W.J., Van Eldik, L.J., 1991. Neurotrophic protein S100 beta stimulates glial cell proliferation. Proc. Natl. Acad. Sci. U S A 88, 3554–3558.
Sonsalla, P.K., Wong, L.Y., Winnik, B., Buckley, B., 2010. The antiepileptic drug zonisamide inhibits MAO-B and attenuates MPTP toxicity in mice: clinical relevance. Exp. Neurol. 221, 329–334.
Tadimalla, A., Belmont, P.J., Thuerauf, D.J., Glassy, M.S., Martindale, J.J., Gude, N., Sussman, M.A., Glembotski, C.C., 2008. Mesencephalic astrocyte-derived neurotrophic factor is an ischemia-inducible secreted endoplasmic reticulum stress response protein in the heart. Circ. Res. 103, 1249–1258.
Tanaka, J., Toku, K., Matsuda, S., Sudo, S., Fujita, H., Sakanaka, M., Maeda, N., 1998. Induction of resting microglia in culture medium devoid of glycine and serine. Glia 24, 198–215.
Tanaka, J., Toku., K., Zhang, B., Ishihara, K., Sakanaka, M., Maeda, N., 1999. Astrocytes prevent neuronal death induced by reactive oxygen and nitrogen species. Glia 28, 85–96.
Van Eldik, L.J., Wainwright, M.S., 2003. The Janus face of glial-derived S100B: beneficial and detrimental functions in the brain. Restor. Neurol. Neurosci. 21, 97–108.
Voutilainen, M.H., Bäck., S., Pörsti, E., Toppinen, L., Lindgren, L., Lindholm, P., Peränen, J, Saarma, M., Tuominen, R.K., 2009. Mesencephalic astrocyte-derived neurotrophic factor is neurorestorative in rat model of Parkinson's disease. J. Neurosci. 29, 9651–9659.
Yano, R., Yokoyama, H., Kuroiwa, H., Kato, H., Araki, T., 2009. A novel anti-Parkinsonian agent, zonisamide, attenuates MPTP-induced neurotoxicity in mice. J. Mol. Neurosci. 39, 211–219.
Yasuhara, T., Shingo, T., Muraoka, K., Kameda, M., Agari, T., Wen, Ji, Y., Hayase, H., Hamada, H., Borlongan, C.V., Date, I., 2005. Neurorescue effects of VEGF on a rat model of Parkinson's disease. Brain Res. 1053, 10–18.
Yasuhara, T., Shingo, T., Kobayashi, K., Takeuchi, A., Yano, A., Muraoka, K., Matsui, T., Miyoshi, Y., Hamada, H., Date, I., 2004. Neuroprotective effects of vascular endothelial growth factor (VEGF) upon dopaminergic neurons in a rat model of Parkinson's disease. Eur. J. Neurosci. 19, 1494–1504.
Yokoyama, A., Sakamoto, A., Kameda, K., Imai, Y., Tanaka, J., 2006. NG2 proteoglycan-expressing microglia as multipotent neural progenitors in normal and pathologic brains. Glia 53, 754–768.
Yokoyama, H., Uchida, H., Kuroiwa, H., Kasahara, J., Araki, T., 2011. Role of glial cells in neurotoxin-induced animal models of Parkinson's disease. Neurol. Sci. 32, 1–7.
Zhao, Y., Kiningham, K.K., Lin St, S.M., Clair, D.K., 2001. Overexpression of MnSOD protects murine fibrosarcoma cells (FSa-II) from apoptosis and promotes a differentiation program upon treatment with 5-azacytidine: involvement of MAPK and NFkappaB pathways. Antioxid. Redox Signal. 3, 375–386.

Coadministration of Domperidone Increases Plasma Levodopa Concentration in Patients With Parkinson Disease

Noriko Nishikawa, MD, Masahiro Nagai, MD, Tomoaki Tsujii, MD, Hirotaka Iwaki, MD, Hayato Yabe, MD, and Masahiro Nomoto, MD, PhD

Objectives: The aim of this study was to examine the effects of the peripheral dopamine D2-receptor antagonist, domperidone, on the plasma kinetics of levodopa in patients with Parkinson disease (PD).

Methods: In a randomized crossover design, 18 hospitalized patients with PD received a single dose of levodopa/benserazide, 100/25 mg, with or without domperidone, 10 mg, under fasting conditions. Plasma levodopa concentrations were determined up to 3 hours after dose administration.

Results: Mean ± SEM levodopa maximum plasma concentration (C_{max}) (14.1 ± 2.9 vs 9.7 ± 1.6 μmol/L; $P < 0.01$), plasma concentration at 30 min ($C_{30\ min}$) (13.7 ± 3.0 vs 8.1 ± 2.0 μmol/L; $P < 0.01$), and area under the plasma concentration-time curve from 0 to 3 hours ($AUC_{0-3\ hr}$) (15.9 ± 3.1 vs 12.1 ± 2.4 μmol/L · hour; $P < 0.05$) were significantly higher after coadministration of levodopa with domperidone compared to levodopa alone. Thus, domperidone increased levodopa C_{max} and $AUC_{0-3\ hr}$ by 1.5- and 1.3-fold, respectively. There were no exacerbations of PD by concomitant domperidone administration.

Conclusions: The results demonstrate that coadministration of domperidone increased the bioavailability of levodopa. This may be the reason for no exacerbation of PD in concomitant administration of domperidone, a dopamine D2-receptor blocker.

Key Words: levodopa, domperidone, pharmacokinetics, Parkinson disease

(*Clin Neuropharm* 2012;35: 182–184)

Domperidone is a peripheral dopamine D2-receptor antagonist that stimulates gastric motility and thereby relieves symptoms associated with gastrointestinal (GI) disease or drug administration, such as nausea, vomiting, and abdominal discomfort.[1] Compared with other D2-receptor antagonists, domperidone passes through the blood-brain barrier (BBB) less readily and is thus associated with a lower risk of central nervous system effects, such as drug-induced parkinsonism.[1] Because of this characteristic, domperidone is commonly used in patients with Parkinson disease (PD) to prevent nausea and vomiting induced by antiparkinsonian drugs.[1–3] Metoclopramide, another D2-receptor antagonist GI prokinetic agent, is known to increase GI motility and accelerate gastric emptying, leading to the promotion of GI absorption, shortened time to onset of action, and increased blood concentrations of concomitantly administered medications.[4] Metoclopramide has lower molecular weight and higher lipophilicity than domperidone and therefore more readily passes through the BBB and induces extrapyramidal symptoms.[3] Administration of metoclopramide to PD patients and the elderly should thus be performed with prudence. Domperidone has been reported to have no statistically significant effect on plasma levodopa disposition in patients with PD[5] and in healthy subjects.[6] The objective of this study was to examine whether domperidone increases the bioavailability of concomitant drugs by comparing the pharmacokinetics of levodopa administered with and without domperidone in patients with PD.

MATERIALS AND METHODS

The study was conducted after approval by the Clinical Research Ethics Committee at Ehime University Hospital. All procedures were consistent with the Declaration of Helsinki.

The study included 18 patients with PD who were hospitalized for treatment at our institution and had not received domperidone during their treatment course. The patients were randomly assigned to receive a single tablet of combined levodopa/benserazide, 100/25 mg, either with or without domperidone, 10 mg. After a 5-day washout, the patients were crossed over to the alternate treatment. All other drugs used for the treatment of PD were continued unchanged during the study. No patients were receiving agents that might alter drug absorption such as metoclopramide, itopride, mosapride, trimebutine, H_2-blockers, and proton pump inhibitors. All medications were administered with adequate water intake under fasting conditions in the early morning. Venous blood samples were drawn immediately before oral administration (time zero) and 30, 60, 90, 120, and 180 minutes after administration into heparinized polypropylene tubes. Samples were centrifuged at 3000 rpm for 15 minutes to obtain plasma, which was stored at −20°C until assayed. All adverse events that were observed by the investigators or reported by the patients in response to indirect questioning were recorded.

Plasma levodopa concentrations were measured using high-performance liquid chromatography (HPLC) with electrochemical detection. Plasma aliquots (100 μL) were mixed with 500 μL of ice-cold 0.2-mol/L perchloric acid containing 0.1-mmol/L EDTA and 5 μL of 15 pg/mL 3,4-dihydroxybenzamine. Samples were centrifuged at 20,000*g* for 15 minutes at 4°C (Himac CF16RX; Hitachi Ltd, Tokyo, Japan). The supernatant was filtered through a 0.45-μm membrane filter (Chromatodisc 4A, GL Science Inc, Tokyo, Japan), and a 10-μL aliquot of the filtered solution was injected into the HPLC system with an electrochemical detector. The HPLC system included a delivery pump, a degasser, and an electrochemical detector (HTEC-500; Eicom, Kyoto, Japan) with a Gilson 234 autoinjector (Eicom). Analytical separation was performed on a reverse-phase column (C18 phase; 150 × 2.1 mm; EICOMPAK SC-5ODS, Eicom) at 30°C. The mobile phase consisted of 12% (vol/vol) methanol containing 0.1-mol/L phosphate buffer

Department of Neurology and Clinical Pharmacology, Ehime University Hospital and School of Medicine, Shitukawa Tohon Ehime, Japan.

Conflicts of Interest and Source of Funding: The authors have no conflicts of interest to declare.

This study was supported by a grant-in-Aid from the Research Committee of CNS Degenerative Diseases, the Ministry of Health, Labor and Welfare of Japan, and SRF, and a grant of Ehime University.

Address correspondence and reprint requests to Noriko Nishikawa, MD, Department of Neurology and Clinical Pharmacology, Ehime University Hospital and School of Medicine, Shitukawa Tohon Ehime 791-0295, Japan; E-mail: n-nishi@m.ehime-u.ac.jp

DOI: 10.1097/WNF.0b013e3182575cdb